Multi-omics analysis uncovers tumor ecosystem dynamics during neoadjuvant toripalimab plus nab-paclitaxel and S-1 for esophageal squamous cell carcinoma: a single-center, open-label, single-arm phase 2 trial

Guoqing Zhang,[a,f] Jing Yuan,[b,f] Chaohu Pan,[c,f] Qing Xu,[d] Xiaoli Cui,[c] Jing Zhang,[a] Minglu Liu,[e] Zhigang Song,[b] Liangliang Wu,[f] Dongfang Wu,[c] Haitao Luo,[c,*] Yi Hu,[a,**] Shunchang Jiao,[a,***] and Bo Yang[g,****]

[a]Department of Oncology, Senior Department of Oncology, the Fifth Medical Center of Chinese PLA General Hospital, Beijing, China
[b]Department of Pathology, the First Medical Center of Chinese PLA General Hospital, Beijing, China
[c]Shenzhen Engineering Center for Translational Medicine of Precision Cancer Immunodiagnosis and Therapy, YuceBio Technology Co., Ltd, Shenzhen, China
[d]Department of Nutrition, the First Medical Center of Chinese PLA General Hospital, Beijing, China
[e]Outpatient Department, Jingnan Medical Area, Chinese PLA General Hospital, Beijing, China
[f]Institute of Oncology, Senior Department of Oncology, the Fifth Medical Center of Chinese PLA General Hospital, Beijing, China
[g]Department of Thoracic Surgery, the First Medical Center of Chinese PLA General Hospital, Beijing, China

eBioMedicine
2023;90: 104515
Published Online xxx
https://doi.org/10.1016/j.ebiom.2023.104515

Summary

Background Immune checkpoint inhibitors combined with chemotherapy as a neoadjuvant therapy have been applied to the treatment of esophageal squamous cell carcinoma (ESCC). However, the optimal regimen needs to be further explored, particularly for older patients, and the mechanisms by which the immune checkpoint inhibitor combined with chemotherapy modulates the evolution of ESCC are unknown.

Methods In this single-arm phase 2 trial, patients with resectable (stage II/III/IV without metastasis) ESCC were enrolled and received nanoparticle albumin-bound (nab) paclitaxel for two cycles and oral S-1 for 2 weeks, combined with intravenous toripalimab for two cycles before surgery. Combination postoperative adjuvant therapy was administered. The primary outcome was the major pathological response (MPR). Secondary outcomes included pathological complete response (pCR), overall response rate (ORR), disease control rate (DCR), disease-free survival (DFS), overall survival (OS), improvement in Stooler's dysphagia score and degree of daily living ability (dADL). Biopsies and plasma pre- and post-neoadjuvant therapy were performed using whole-exome sequencing, transcriptome sequencing, immunohistochemistry (IHC) for PD-L1, multiplex immunofluorescence (mIF) and proximity extension assay technology (PEA) for 92 proteins.

Findings From November 2019 to July 2021, 60 patients were enrolled. After neoadjuvant therapy, R0 resection was achieved in 55 (98.21%) patients. MPR was identified in 27 patients (49.09%), and 16 patients (29.09%) achieved pCR. Patients with PR, SD and PD were 37 (61.67%), 21 (35.00%) and 2 (3.33%), respectively. The overall staging, Stooler dysphagia scores and dADL were significantly decreased after treatment. 11 patients (18.3%) experienced grade ≥3 AEs. Compared to PD-L1-Low patients, PD-L1-High patients had a significantly higher ratio of PR. During therapy, the tumor mutation burden (TMB) and tumor neoantigen burden (TNB) were significantly decreased in patients with PR. Differential clonal evolution within tumors was demonstrated by analysis of intratumoral heterogeneity. Transcriptome analyses revealed that the infiltration of CD4+ T lymphocytes at baseline was associated with clinical outcome. During therapy, CD8+ T cells and CD4+ T cells were increased in all patients; however, exhausted cells, nTregs and iTregs were significantly increased in patients with non-MPR. Protein analyses revealed that the levels of IFN-γ, Gal.1 and LAMP3 can predict the clinical benefit. In addition, the expression of CD83, TNFRSF4, TNFSF14, VEGFR2, ADA, ARG1, and HO-1 was associated with serious AEs. More importantly, the integration of CD4+ T cells with plasma protein of IFN-γ, Gal.1 or LAMP3 could further distinguish responders from non-responders.

*Corresponding author.
**Corresponding author.
***Corresponding author.
****Corresponding author.
E-mail addresses: luohaitao@yucebio.com (H. Luo), huyi301zlxb@sina.com (Y. Hu), jiaoshunchang@csco.org.cn (S. Jiao), yangbotmmu@301.com (B. Yang).
[f]These authors contributed equally to this work.

Interpretation In this study, neoadjuvant therapy with toripalimab, nab-paclitaxel and S-1 was less toxic and showed promising antitumor activity in patients with resectable ESCC. Changes in the genome, transcriptome, PD-L1 expression and serum proteins were comprehensively analyzed and correlated with clinical outcomes, which provides insight into the mechanism of action of toripalimab combined with nab-paclitaxel and S-1 in patients with ESCC.

Funding This study was funded by Major projects of the ministry of science and technology of the 13th five-year plan of China [grant number: 2018ZX09201013].

Keywords: Esophageal squamous cell carcinoma; Neoadjuvant therapy; PD-L1; TMB; CD4 T cells; Serum proteins

Research in context

Evidence before this study

Immune checkpoint inhibitors (ICIs) in combination with platinum-based chemotherapy has been approved as first-line treatment for locally advanced or metastatic esophageal cancers. However, platinum-based regimens are highly toxic. S-1 is considered to be less toxic and tolerable in patients with esophageal cancer compared to platinum-based drugs, and chemoradiotherapy with S-1 has a significant benefit over radiotherapy alone in elderly patients with esophageal cancer. Therefore, there is an urgent need to evaluate the efficacy and safety of neoadjuvant therapy ICIs combined with S-1 chemotherapy regimens.

Added value of this study

In this single-arm phase 2 trial, neoadjuvant therapy toripalimab combined with nab-paclitaxel and S-1 in resectable ESCC had a lower incidence of treatment-related serious AEs (18.3%) with pCR and MPR of 29.09% and 49.09%, respectively. The overall staging, Stooler dysphagia scores and dADL were significantly decreased after treatment. Prognostic biomarkers and tumor ecosystem dynamics during neoadjuvant treatment were analyzed. An association between changes of TMB and TNB with response during treatment was observed. Neoadjuvant therapy can alter the tumor microenvironment and promote the infiltration of CD4 and CD8 T lymphocytes. However, the number of immunosuppressive cells also increased in non-responders. Furthermore, PD-L1 expression, CD4 T cells and serum levels of IFN-γ, LAMP3 and Gal.1 could predict the efficacy of neoadjuvant treatment. More importantly, the combination of CD4 T cells and serum levels of IFN-γ, LAMP3 or Gal.1 could further distinguish responders from non-responders.

Implications of all the available evidence

This study highlights the safety and efficacy of toripalimab combined with nab-paclitaxel and S-1 in patients with resectable ESCC, indicating that this regimen is a potential treatment strategy for such patients. Biomarkers for response were identified, and the tumor and microenvironment ecosystem dynamics were clarified. While further studies are needed to validate these findings.

Introduction

Esophageal cancer is mainly divided into squamous cell carcinoma (SCC) and adenocarcinoma, which was responsible for 544,000 deaths in 2020, ranking sixth among all cancers.[1] Esophageal squamous cell carcinoma (ESCC) has the highest incidence in Southeast Asia.[2] Most patients with ESCC are diagnosed at localized or locoregional stages, and surgery remains an effective treatment choice for these patients.[3] However, the R0 resection rate is approximately 50% in locally advanced ESCC and the early recurrence rate is high after surgery.[4,5] Although neoadjuvant therapy, such as chemotherapy or chemoradiotherapy, has improved the rate of R0 resection and survival, the clinical benefit remains suboptimal and unsatisfactory.[6–8] Therefore, more effective neoadjuvant therapy is urgently required to improve the clinical outcomes of patients with ESCC.

Immune checkpoints, such as PD-1 and CTLA4, inhibit the proliferation and activation of T lymphocytes by binding to ligands, and ultimately downregulating the anti-tumor immune response.[9,10] However, immune checkpoint inhibitors (ICIs) can inhibit the effect of immune checkpoints on T lymphocytes and enhance anti-tumor immunity.[11] Currently, ICIs are used for the treatment of various cancers, including ESCC.[12,13] The ICIs pembrolizumab and nivolumab have been approved by the FDA for the second-line treatment of patients with advanced ESCC.[14,15] With an improved understanding of the antitumor mechanism, it has been found that the combination of immunotherapy and chemotherapy may achieve synergistic effects.[16] This may be due to the role of chemotherapy to promote the immunogenic death of tumor cells, change the tumor microenvironment, and ultimately improve

the antitumor effect of ICIs.[17,18] Pembrolizumab in combination with platinum-based chemotherapy has been approved as a first-line treatment for locally advanced or metastatic esophageal cancer that is unresectable or unsuitable for radical chemotherapy.[19] However, platinum-based therapies are highly toxic and can cause approximately 40 specific adverse effects.[20] Indeed, at ESMO 2019, Lee et al. reported that eight deaths (28.6%) occurred after preoperative administration of pembrolizumab plus platinum-based chemoradiotherapy, two resulting from pre-surgical hematemesis, two due to acute lung injury, and four resulting from disease progression.[21] Therefore, a more effective and less toxic neoadjuvant treatment regimen is urgently needed, particularly for older patients. Compared to platinum drugs, S-1 is considered less toxic and tolerable in patients with esophageal cancer, and chemoradiotherapy with S-1 provides significant benefits over radiotherapy alone in older patients with esophageal cancer. Therefore, the efficacy and safety of neoadjuvant therapy ICIs combined with the S-1 chemotherapy regimen instead of platinum-based chemotherapy are urgently required.

Tumor genomic features and the tumor microenvironment have been reported to be associated with the response to ICIs treatment.[22,23] PD-L1 expression and tumor infiltrating lymphocytes (TILs) status have been reported to be associated with overall survival in ESCC patients treated with ICIs.[12] However, the dynamics changes in the tumor genome, tumor microenvironment and plasma proteins induced by ICIs combined with chemotherapy in patients with ESCC are unclear. The analysis of such changes may improve understanding of the antitumor effects of ICIs combined with chemotherapy in patients with ESCC to identify potential predictive or prognostic biomarkers.

In this study, we performed a single-arm phase 2 trial to evaluate the efficacy and safety of neoadjuvant therapy toripalimab combined with nab-paclitaxel and S-1 for ESCC and to identify predictive or prognostic biomarkers as well as to reveal the dynamics of the tumor ecosystem during treatment.

Methods

Study design and population

This single center, single arm, phase 2 clinical trial of neoadjuvant toripalimab, combined with nab-P and S-1 in ESCC was performed at the First Medical Center of the Chinese PLA General Hospital. Between November 2019 and July 2021, patients diagnosed with ESCC who were considered eligible for surgical treatment were enrolled.

Patients were considered eligible if they met the following inclusion criteria: (1) aged ≥18 years, (2) histologically confirmed stage II/III/IV ESCC without metastasis, (3) confirmed tumor resectability, (4) considered by the physician to be able to endure the surgery process, (5) had received no prior systemic therapy, (6) ECOG PS scores of 0 and 1, (7) negative result for urine pregnancy test and (8) able to read and understand the information present in the informed consent form. Patients were excluded if they (1) had aortic and tracheal invasion (T4), (2) previously received treatment targeting PD-L1, PD-L2, PD-1, CTLA4, OX40 or CD137 (3) had active autoimmune disease or immunodeficiency, (4) received a vaccine within 30 days prior to enrollment and (5) had severe disorders in the liver, kidney, heart, endocrine, or circulatory system.

Biopsies and plasma from pre- and post-neoadjuvant therapy were collected and performed with whole-exome sequencing (WES), transcriptome sequencing, immunohistochemistry (IHC) for PD-L1, multiplex immunofluorescence (mIF) and proximity extension assay technology (PEA) for 92 proteins.

Ethics

This study was conducted according to the guidelines of the Ethics Committee of the General Hospital of the People's Liberation Army and written informed consent was obtained from all participants. The clinical Trial registration number was ChiCTR1900027160.

Interventions

Neoadjuvant therapy consisted of intravenous nanoparticle albumin-bound (nab) paclitaxel 260 mg/m^2 for two cycles (D1, Q3W), oral tiggio capsule (S-1) 40–60 mg/time (D1-14, bid, Q3W) for 2 weeks and 240 mg of intravenous toripalimab for two cycles (D4, Q3W). Surgery was planned to begin within 4 weeks of neoadjuvant therapy. All patients would undergo thoracic laparoscopy combined with radical resection for esophageal cancer. Postoperatively, the patients received combination adjuvant therapy with nab-paclitaxel, tiggio and toripalimab for four cycles (using the same principle as preoperative dosing). The addition of radiation therapy (RT) to combination adjuvant therapy was performed according to the TNM classification.[24] Toripalimab treatment was discontinued during the RT. Adjuvant radiotherapy is spared, but individualized treatment is performed according to the effect of neoadjuvant therapy, pathological stage and individual intention. Radical radiotherapy is recommended for patients without R0 excision. For patients with recurrence and progression, the decision of radical radiotherapy will be made according to the site of recurrence, tumor spread and personal physical condition. Intensity modulated radiotherapy (IMRT) was used for radiotherapy. For R0 resection patients, postoperative adjuvant radiotherapy regimen was 45–50.4Gy (1.8–2.0Gy/day), 5 times a week (total 25–28 fractions). For patients with R1/2 resection and patients with local recurrence (anastomotic or septal lymph nodes), the regimen of radical

radiotherapy was 95% planing target volume (PTV) 50Gy (1.8–2.0Gy/d), followed by 95% planing gross target volume (PGTV) 10Gy (1.8–2.0Gy/d), 5 times a week. After combination adjuvant therapy or radiation therapy, patients were administered 240 mg of intravenous toripalimab for 6 months (Q3W).

Study outcomes

The primary outcome was major pathological response (MPR), defined as ≤10% of viable tumor remaining within the primary tumor bed after neoadjuvant treatment. As secondary outcomes, the pathological complete response (pCR) rate, overall response rate (ORR), disease control rate (DCR), disease-free survival (DFS), overall survival (OS), improvement in Stooler's dysphagia scores and degree of daily living ability (dADL) scores were recorded. The time frame for recording AEs was up to 1 month after the last cycle of neoadjuvant treatment. All eligible patients who received neoadjuvant therapy were included in primary and secondary outcome analyses. The incidence of postoperative complications was evaluated in patients who underwent surgical resection.

IHC and mIF staining

IHC of PD-L1

Formalin-fixed paraffin-embedded (FFPE) tumor biopsies pre- and post-treatment were collected and the PD-L1 combined positive score was assessed with a PD-L1 IHC assay according to the manufacturer's instructions.[25] The samples were considered PD-L1-Hign if CPS ≥10.

mIF staining

Four samples were subjected to the mIF staining from patients of P03 and P34. The 5 μm-thick slides cut from the FFPE blocks were dewaxed with xylene. Then the slides were rehydrated with a decreasing ethanol series. After rehydrating, the slides were fixed with 10% neutral buffered formalin for 10 min. Next, the slides were stained with markers of CD8, Foxp3 and Pan cytokeratin (Cat# OP-000001, akoyo biosciences), followed by incubation with blocking proteins for 10 min. After blocking, the slides were incubation with horseradish peroxidase (HRP)-conjugated secondary antibody and tyramide signal amplification (TSA). Finally, the slides were stained with 4′-6′-diamidino-2-phenylindole (DAPI) for 10 min and images were acquired with vectrapolaris (akoyo biosciences).

Next-generation sequencing and data analysis

WES

FFPE tumor biopsies and matched peripheral blood samples were performed with the GeneRead DNA FFPE Kit (QIAGEN, GER) and Mag-Bind® Blood & Tissue DNA HDQ 96 Kit (OMEGA), respectively. The extracted DNA was quantified using the Qubit dsDNA HS Assay Kit (Thermo Fisher Scientific, USA). Sequencing libraries were built with Exome Plus Panel V1.0 (IDT, USA). Sequencing was performed using the MGISEQ platform. The median depth of coverage was 293.7 × for tumor tissue specimens and 158.79 × for whole blood control samples.

Data processing

Sequencing data were analyzed using SOAPnuke (v1.5.6) to filter out reads with low quality and an N rate beyond 10%.[26] The clean reads were mapped to the human reference genome hg19 with the Burrows-Wheeler Alignment tool (version 0.7.12).[27] SAMtools (version 1.3) was used to perform alignment data conversion, sorting, and indexing.[28] Duplicates were removed with SAMBLASTER (Version 0.1.22) to reduce the bias.[29]

Somatic mutation analysis

Somatic mutations were identified with VarDict (1.7.0), including single nucleotide variants (SNVs) and insertions and deletions (indels).[30] Both SNVs and indels with a low variant allelic fraction (VAF <0.009) or a low total read coverage (<6 reads for tumor samples; <3 reads for germline samples) were filtered out. The identified mutation was annotated with SnpEff software (Version 4.3).[31] The tumor mutation burden (TMB) was defined as the number of non-synonymous somatic mutations per megabase based on the exome examined. The cut-off values for TMB-High and TMB-Low were defined as the median values of TMB.

Calculation of tumor neoantigen burden (TNB)

The TNB levels were determined as previously described.[32] In brief, human leukocyte antigens (HLA) from tumor tissue specimens and matched whole blood control samples were typed with POLYSOLVER (v1.0) and OptyType (v1.3.2).[33] LOHHLA software was used to calculate HLA deletion.[34] Then, in-house software centered on mutated amino acids was used to translate all non-synonymous mutations and indels into 21-mer peptide sequences. The translated 21-mer peptide was then used to produce a 9- to 11-mer peptide with a sliding window approach, which was used to predict the binding affinity of MHC class I. NetMHCpan (v3.0) was used to predict the binding strength of mutated peptides to HLA alleles.[35] The peptide was selected if the predicted binding affinity of peptides to HLA alleles with half-maximum inhibitory concentration (IC50) was ≤500 nM. The TNB was defined as the number of putative neoantigens per megabase on the genome examined. The median values of TNB were used as cut-off value for dividing high and low.

Evaluation of HLA LOH and microsatellite instability (MSI)

The types of HLA in the tumor tissue and matched peripheral blood samples were determined with

OptyType (v1.3.2) and POLYSOLVER (v1.0).[33,36] The LOHHLA software was used to determine the maintenance or loss of HLA.

The MSI status was detected with MSIsensor (v0.2).[37] An in-house tool was then used to recalculate and correct MSI value.

Tumor clonality analysis

The number of clones and cellular prevalence of inferred mutational clusters in each tumor sample were calculated with PyClone (v0.13.1).[38] For patients with paired pre- and post-samples, variants were considered to indicate gained variants if they were identified only in the post-treatment sample and did not occur in the pre-treatment sample. Variants indicating lost variants occurred only in the pre-treatment sample but not in the post-treatment sample. Variants with a higher number post-treatment than pre-treatment were defined as increased variants. Variants with a lower number post-treatment than pre-treatment were defined as decreased variants.

RNA sequencing

Total RNA of tumor samples was isolated from the tumor tissue with RNeasy Plus Universal Kits (Qiagen, GER) according to the manufacturer's instructions. A Qubit™ RNA HS Assay Kit (Thermo Fisher Scientific, USA) was used to quantify the concentrations of the extracted RNA. The purity and integrity of the RNA were checked with Take 3 (BioTek, USA) and the RNA Cartridge kit of the Qseq100 Bio-Fragment Analyzer (Bioptic, CHN), respectively. The VAHTS mRNA-seq V3 Library Prep Kit for Illumina (Vazyme, CHN) was used to construct RNA-seq libraries. Finally, the libraries were sequenced on the NextSeq 550AR with 150 bp paired-end reads.

Gene expression analysis

Raw sequencing data were processed to filter out low-quality reads and adapters using trim galore (0.6.7). The reads counts and transcripts per million (TPM) values were calculated using Kallisto (v0.46.2), which pseudoaligned sequencing reads to reference transcripts downloaded from Gencode (v38) database.[39] The gene expression level was normalized to TPM. The reads counts matrix was used to identify differentially expressed genes (DEGs) by the DESeq2 package.[40] DEGs with |log2FoldChange| > 1, and *P*-value < 0.01 were considered as significant DEGs. The ggpubr and Complexheatmap R package were used to generate volcano and heatmap plots, respectively. Kyoto Encyclopedia of Genes and Genomes (KEGG) pathway enrichment was performed with KOBAS-i web tool with a *P*-value < 0.05.[41] The median values of gene expression were used as cut-off value for dividing high and low.

Immune-related signature and infiltration abundance of immune cells analysis

A gene expression matrix was used to calculate the score of immune-related signatures with Riaz's algorithms[42] and the enrichment level of 12 major infiltrating lymphocytes with ImmuCellAI.[43] The median values of different lymphocytes were used as cut-off value for dividing high and low.

PEA

Plasma blood samples were collected and analyzed using the Olink® immune oncology panel* (Olink Proteomics AB, Uppsala, Sweden) to measure the levels of 92 proteins according to the manufacturer's instructions. This technology is based on the PEA.[44] Briefly, pairs of oligonucleotide-labeled antibodies bind to each target protein. If the two antibodies are in close proximity, the oligonucleotides will hybridize in a pairwise manner. The addition of DNA polymerase generates a unique PCR target sequence, which is formed through proximity-dependent DNA polymerization. The generated DNA sequence was detected and quantified with a microfluidic real-time PCR instrument (Biomark HD, Fluidigm). Then a set of internal and external controls were used for quality control and to normalize the resulting Ct-data. The final results were presented as normalized protein expression (NPX) values.

The internal controls were designed to mimic and monitor the different steps of PEA, and these controls were introduced to all samples. They consisted of two incubation/immuno controls, an extension control and a detection control. The internal controls and the external controls are used for quality control and normalization of the data. The external controls consisted of a negative control that was used to calculate the limit of detection (LOD), as well as triplicate interplate controls (IPCs) that were used for normalization of data. Quality control of the data was performed in two steps. First, the run was quality controlled by calculating the standard deviation for the detection control and the incubation/immuno controls. The standard deviation should be below 0.2 for a run to pass the quality control. Second, each sample was quality controlled by comparing the results for the detection control and one of the incubation controls against the run median. Samples that fall more than 0.3 NPX from the run median with regard to these two internal controls are considered to have failed quality control. The median value of protein level was used as cut-off value for dividing high and low.

Statistical analysis

In 2016, F. Klevebro et al. reported that the proportion of residual tumor cells ≤10% after neoadjuvant chemotherapy for esophageal cancer was 15% (12/78), and SCC was 26% (5/19).[45] In 2017, M. C. J. Anderegg et al.

reported in a retrospective study that pCR and PR after neoadjuvant chemotherapy for esophageal cancer were 6.9% (9/131) and 29% (38/131), respectively.[46] Based on these results, the MPR of neoadjuvant chemotherapy for esophageal cancer is estimated to be about 22%. The treatment regimen in this study is expected to increase MPR by 46%.

The PASS15 software with exact test method is used to calculate the sample size and set $\alpha = 0.05$ (two-sided) and $\beta = 0.20$. The enrollment duration is 12 months (November 2019 and October 2020) and the follow-up time is 36 months. To detect the difference between A and B with 80% power, at least 27 subjects need to be enrolled. Considering the 10% dropout rate, the estimated sample size is 30. At the ESMO meeting in 2021, we report the progress of this study with an MPR of 50%.[47] Based on this encouraging result, we intend to add approximately 30 patients to further study additional exploratory results.

All statistical analyses were performed using the R software version 4.1.2. The baseline characteristics of patients are expressed as number (percentage) for categorical variables, mean ± SD for normally distributed variables and median (IQR) for non-normally distributed variables. Safety and efficacy analyses of neoadjuvant therapy were performed on the intention-to-treat (ITT) population. And the analysis of the relationship between molecular markers and treatment efficacy was performed on the per-protocol Set. The t-test were used to compare differences between groups. Categorical variables were evaluated with Fisher's exact test. Correlation analysis was conducted using Pearson correlation analysis. When the correlation coefficient is ≥ 0.8, it is defined as strong correlation. Correlation coefficient 0.6 is the cut-off value of moderate correlation and low correlation. The significance of OS, PFS and DFS were analyzed with Kaplan–Meier curve analysis. The dependent and independent variables for statistical tests have been listed in Table S1. Under the assumption of missing at random, missing data was not included in the relevant analysis. Statistical significance was set at $P < 0.05$.

Role of the funding source

The funders have no role in the study design, the data collection, data analysis, interpretation, and the writing of the report. The corresponding author had full access to all of the data and the final responsibility to submit for publication.

Results

Overview of patient cohort

Between November 2019 and July 2021, 67 patients were screened for eligibility, among whom, 60 patients were enrolled and administered neoadjuvant therapy (Fig. 1A). 1 patient had severe atrial fibrillation during treatment, and 3 patients withdrew consent of surgery. After neoadjuvant therapy, 56 patients underwent surgery and R0 resection was achieved in 55 patients. A total of 11 patients received adjuvant radiation therapy (Table S2). The baseline demographic and clinical characteristics of the patients are shown in Table 1. The median age of all patients was 60.9 (range 45–75) years. Most patients were male (85.00%), stage III-IV without metastasis and with lymph node involvement (83.33%). The histological characteristics and tumor locations varied between patients. Pre- and post-treatment biopsies and plasma were collected and subjected to WES, transcriptome sequencing, IHC for PD-L1, mIF and PEA technology for 92 proteins. Then the association between the results from multi-omics and clinical outcomes was analyzed (Fig. 1B).

Efficacy and safety of neoadjuvant treatment

After neoadjuvant (preoperative) treatment, 55 (98.21%) patients achieved R0 resection (Fig. 1A). The time from diagnosis and latest neoadjuvant therapy to surgery was 94 (76.5, 125.5) and 27 (19.5, 35.0) days, respectively. The surgery duration was 310.0 (285.8, 356.0) min for 55 patients. The intraoperative blood loss was 100 (100, 200) mL and the surgical difficulty was 78.18%, 16.36%, and 5.45% for 1, 2, and 3, respectively. Seventeen (30.91%) patients presented complication events, including hoarseness (11, 18.33%), pulmonary infections (4, 6.67%), anastomotic fistula (3, 5.45%), cough (2, 3.64%) and atrial fibrillation (1, 1.82%) (Table 2 and Table S3).

According to the criteria of RECIST 1.1, the CR, PR, SD and PD rates were 0, 61.67%, 35.00% and 3.33%, respectively, yielding a DCR of 96.67% in all patients (Fig. 1C and D and Table 3). Twenty-seven patients (49.09%) experienced MPR, sixteen (29.09%) experienced pCR, thirty-eight (69.09%) experienced ≥50% pathologic regression and fifty-one patients (92.73%) achieved downstaging (Fig. 1C and D, Table 3 and Table S2). In addition, the overall staging, Stooler dysphagia scores and dADL scores were significantly decreased after treatment (Fig. 1E–G).

Correlations between major pathological and radiological responses were analyzed. As shown in Table 4, the significant association was only detected between radiological response and ≥50% tumor regression. No correlations were detected between MPR or pCR and the radiologically detected responses.

The treatment–related AEs are summarized in Table 5. The most common AEs were alopecia (93.33%), muscle soreness (73.33%), fatigue (58.33%), anemia (51.67%), leukopenia/neutropenia (51.67%) and peripheral sensory neuropathy (51.67%). Eleven (18.33%) patients experienced serious AEs, including ten (16.67%) patients who experienced grade 3 AEs and one (1.67%) patient who experienced a grade 4 AE. The most frequent

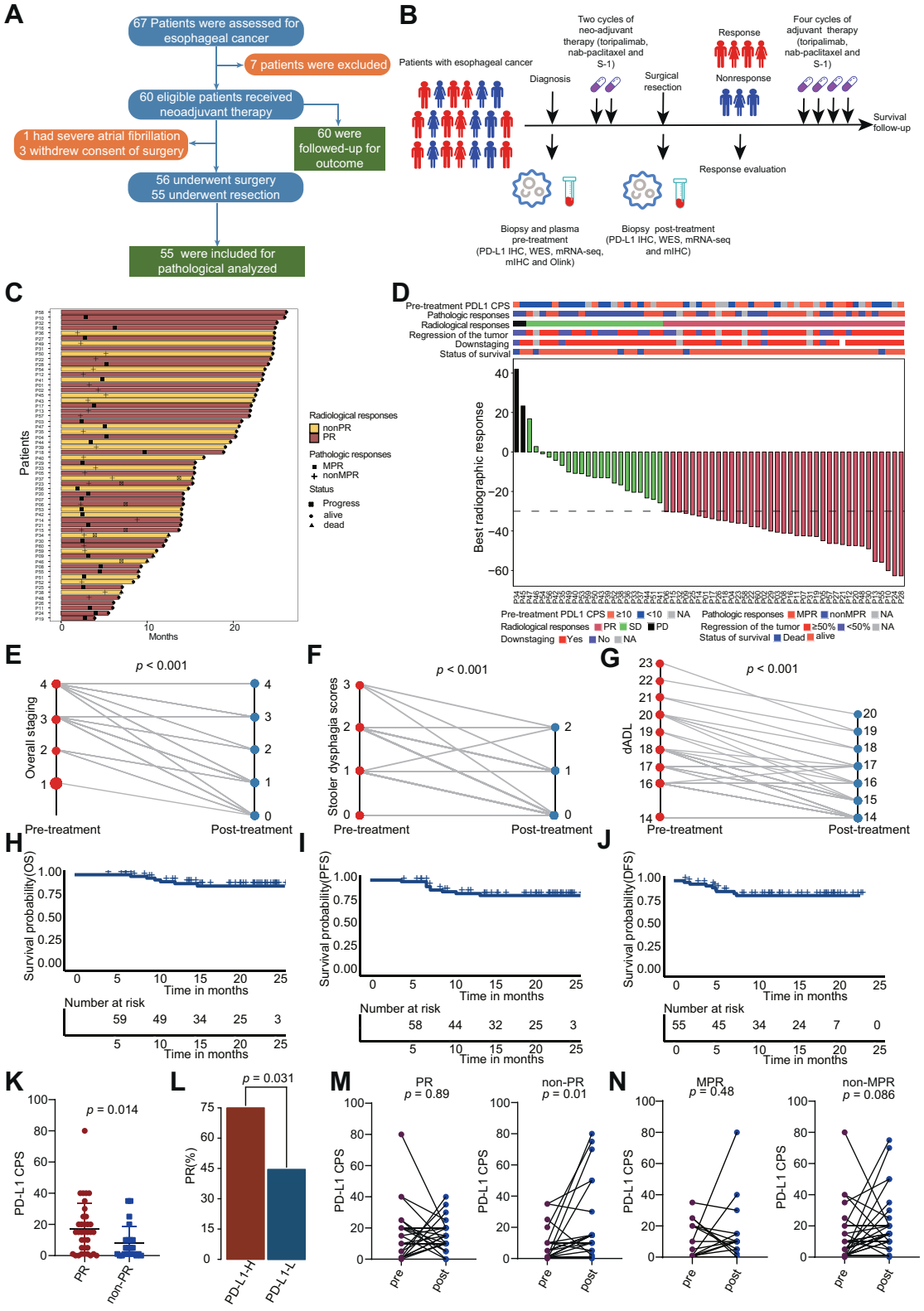

***Fig. 1:* Efficacy and safety of neoadjuvant treatment.** (A) Study flow chart. (B) Overview of the study. (C) Response and duration for the patients with neoadjuvant treatment. (D) Waterfall plots of best radiographic response by RECIST 1.1. (E) Comparative efficacy of neoadjuvant

Characteristics	All patients (n = 60)
Age of diagnose, years	60.9 (45–75)
Male sex	51 (85.00%)
ECOG performance status	
0	34 (56.67%)
1	26 (43.33%)
Stooler's dysphagia score	
0	13 (21.67%)
1	21 (35.00%)
2	23 (38.33%)
3	3 (5.00%)
Histology	
Squamous cell carcinoma	60 (100.00%)
Overall clinical staging	
I	1 (1.67%)
II	9 (15.00%)
III	28 (46.67%)
IV	22 (36.66%)
Preoperative T status	
cT1	3 (5.00%)
cT2	10 (16.66%)
cT3	26 (43.33%)
cT4	21 (35.00%)
Preoperative N status	
cN0	10 (16.67%)
cN1	26 (43.33%)
cN2	19 (31.67%)
cN3	5 (8.33%)
Tumor grade (Differentiation)	
Well	7 (11.67%)
Well-Moderate	2 (3.33%)
Moderate	34 (56.67%)
Moderate-Poor	4 (6.67%)
Poor	13 (21.67%)
Tumor location	
Middle-Upper	1 (1.67%)
Middle	18 (30.00%)
Middle-Lower	22 (36.67%)
Lower	19 (31.67%)

Data are presented as median (range) or n (%). ECOG, Eastern Cooperative Oncology Group; cT, clinical tumor stage; cN, clinical nodal stage.

Table 1: **Baseline clinical characteristics of the study population.**

Characteristics	All patients (n = 55)
Time from diagnosis to surgery, days	94 (76.5, 125.5)
Time from latest neoadjuvant therapy to surgery	27 (19.5, 35.0)
Surgery duration, minutes	310.0 (285.8, 356.0)
Blood loss, mls	100 (100, 200)
Length of stay in hospital, days	14.0 (9.0, 18.0)
Surgery difficulties	
1	43 (78.18%)
2	9 (16.36%)
3	3 (5.45%)
All complications cases	
Anastomotic fistula	3 (5.45%)
Hoarseness	11 (18.33%)
Pulmonary infection	4 (6.67%)
Cough	2 (3.64%)
Dysphagia	3 (5.45%)
Atrial fibrillation	1 (1.82%)
Fever	1 (1.82%)

Data are presented as median (Q1, Q3) or n (%).

Table 2: **Characteristic and complications observed during perioperative period.**

grade 3–4 AEs was leukopenia/neutropenia (Table S3). No treatment related mortalities were observed.

The median OS, PFS and DFS were not reached by the end of the follow-up period at November 18, 2021. The estimated 6 and 12-month OS, PFS and DFS rates were 100%, 93.3%, 98.3%, 86.7%, 89.7% and 86.2% respectively (Fig. 1H–J). Except for DFS in the PR/non-PR group, the OS, PFS and DFS were longer in patients with MPR and PR than in those with nonMPR and nonPR, respectively (Fig. S1A and B).

To determine if PD-L1 expression affects the effect of neoadjuvant therapy, 59 pre-treatment biopsies were performed with IHC. The expression of PD-L1 was significant higher in patients with PR than in those with nonPR, and the rate of PR was significantly higher in patients with CPS ≥10 (Fig. 1K and L and Fig. S1C). However, there was no significant difference in the expression of PD-L1 with OS, PFS and DFS (Fig. S1D). The expression of PD-L1 during treatment was analyzed and it was found that the expression level of PD-L1 was increased in non-responders (Fig. 1M and N). However, there were no significant differences in the response rate, DFS or OS (Fig. S1E–G).

Genomic characteristics of tumors pre- and post-neoadjuvant therapy

To examine tumor genomic characteristics and their potential association with response, 41 pre- and 15 post-treatment biopsies were collected and subjected to WES. The genomic landscape of these patients was shown in

treatment for overall staging. (F) and (G) Comparative efficacy of neoadjuvant treatment for Stooler's dysphagia scores (F) and dADL scores (G). (H) to (J) OS (H), PFS (I) and DFS (J) curve for patients with neoadjuvant treatment. (K) Comparison of PD-L1 CPS between patients with PR and non-PR. (L) Barplots of PR rate between PD-L1-H (CPS≥10) group and PD-L1-L (CPS<10) group. (M) Comparison of PD-L1 CPS pre- and post-treatment in PR and non-PR patients, respectively. (N) Comparison of PD-L1 CPS pre- and post-treatment in MPR and non-MPR patients, respectively.

Characteristics	All patients
Pathologic responses	**(n = 55)**
Major pathological response	
No	28 (50.91%)
Yes	27 (49.09%)
Pathologic complete response	
No	39 (70.91%)
Yes	16 (29.09%)
>50% Regression of the tumor	
No	17 (30.91%)
Yes	38 (69.09%)
Radiological responses	
Downstaging	**(n = 55)**
No	4 (7.23%)
Yes	51 (92.73%)
Overall response	**(n = 60)**
CR	0
PR	37 (61.67%)
SD	21 (35.00%)
PD	2 (3.33%)
Objective response (CR + PR)	
No	23 (38.33%)
Yes	37 (61.67%)
Disease control (CR + PR + SD)	
No	2 (3.33%)
Yes	58 (96.67%)
Symptom response	
Post-treatment Stooler's dysphagia score	
0	46 (76.67%)
1	11 (18.33%)
2	3 (5.00%)
3	0

Table 3: **Summary of treatment efficacy (evaluated at the time of surgery).**

Fig. 2A. At baseline, all patients were MSI-low, with a median TMB and TNB of 4.5/MB and 1.56/MB, respectively. HLA LOH was detected in 24 patients. Common mutations were TP53 (91%), TTN (43%), KMT2D (29%) and NOTCH1 (23%) which were consistent with the findings of previous report.[48] The detailed tumor characteristics are shown in Tables S4–S6.

To identify genomic biomarkers to predict the efficacy in ESCC patients treated with neoadjuvant therapy, TMB, TNB and HLA LOH levels at baseline were analyzed. However, no significant differences were observed between these biomarkers (Fig. 2B, Fig. S2A–I). To study genomic evolution during neoadjuvant therapy, TMB, TNB and tumor clone changes were analyzed. Compared to non-PR patients, TMB and TNB were significantly decreased in PR patients (Fig. 2C and D), consistent with immunoediting. Theoretically, in responders, most clones would disappear or decrease after treatment, and there would be fewer drug-resistant or newly-gained clones; to verify this, we further analyzed the non-synonymous mutations pre- and post-treatment and divided these mutations into four categories: gained, lost, increased and decreased (Fig. 2E and F). In patients with MPR, such as P07 and P21, the ratio of gained plus increased clones pre-post did not exceed 11%. However, in patients with non-MPR, such as P12, P33, P34, P45, and P60, the ratio of gained and increased clones pre-post exceeded 50%. Furthermore, a statistical analysis of the correlation between the clinical benefits and the proportion of non-synonymous mutations was conducted. The results showed that the ratio of gained plus increased clones was lower, while the ratio of lost plus decreased clones was higher in responders than in non-responders (Fig. 2G and H, Fig. S2J and K).

Next, all mutated genes were analyzed to further explore the mechanisms that influenced tumor clonal expansion or shrinkage. A total of 3038 gene mutations with the change in the VAF value consistent with their cluster's cellular prevalence were obtained, including 890 genes involved in clonal expansion, which may lead to tumor resistance, and 2148 genes related to clonal shrinkage, which may confer drug sensitivity to tumors (Fig. 2I). We further analyzed the association of the gene mutation statuses and survival in the TCGA esophageal carcinoma cohort,[49] and found that patients with a mutation in the drug sensitive gene YLPM1 had a longer survival period, while those with mutations in the drug resistance gene CCDC106 had a shorter survival period (Fig. 2J and K).

Transcriptome analysis and changes during neoadjuvant therapy

To study the genes associated with prognosis and gene changes during treatment at the transcriptome level, 27

Pathological outcomes	Radiological Outcomes			*P*-value
	PR	SD	PD	
Major pathological response (n = 27)	20	7	0	0.068
Pathologic complete response(n = 16)	12	4	0	0.29
>50% Regression of the tumor (n = 38)	26	12	0	**0.038**

Data are presented as n .The analysis was performed with Fisher's exact test and significant values are showing in bold. PR, partial response; SD, stable disease; PD, progressive disease.

Table 4: **The association between pathological outcomes and radiological outcomes.**

Adverse events	Any grade	Grade 1	Grade 2	Grade 3	Grade 4
Blood system disorders					
Leukopenia/Neutropenia	31 (51.67%)	14 (23.33%)	10 (16.67%)	6 (10%)	1 (1.67%)
Thrombopenia	6 (10%)	4 (6.67%)	2 (3.33%)	0	0
Anemia	31 (51.67%)	27 (45%)	4 (6.67%)	0	0
Gastrointestinal disorder					
Nausea	27 (45%)	18 (30%)	7 (11.67%)	2 (3.33%)	0
Vomiting	3 (5%)	3 (5%)	0	0	0
Diarrhea	9 (15%)	5 (8.33%)	4 (6.67%)	0	0
General disorders					
Fatigue	35 (58.33%)	32 (53.33%)	3 (5%)	0	0
Fever	7 (11.67%)	7 (11.67%)	0	0	0
Muscle soreness	44 (73.33%)	37 (61.67%)	7 (11.67%)	0	0
Respiratory disorders					
Pneumonitis	3 (5%)	1 (1.67%)	1 (1.67%)	1 (1.67%)	0
Nervous system disorders					
Peripheral sensory neuropathy	31 (51.67%)	27 (45%)	4 (6.67%)	0	0
Metabolism and nutrition disorder					
Anorexia	24 (40%)	24 (40%)	0	0	0
Hyperglycemia	14 (23.33%)	13 (21.67%)	0	1 (1.67%)	0
Skin disorders					
Alopecia	56 (93.33%)	32 (53.33%)	24 (40%)	0	0
Rash	22 (36.67%)	15 (25%)	6 (10%)	1 (1.67%)	0
Endocrine disorders					
Hyper/Hypothyroidism	5 (8.33%)	4 (6.67%)	1 (1.67%)	0	0
Investigations					
AST increased	17 (28.33%)	12 (20%)	4 (6.67%)	1 (1.67%)	0
ALT increased	15 (25%)	12 (20%)	2 (3.33%)	1 (1.67%)	0
Creatinine increased	1 (1.67%)	1 (1.67%)	0	0	0
Serum lipase increased	8 (13.33%)	8 (13.33%)	0	0	0
Electrolyte abnormalities	5 (8.33%)	4 (6.67%)	1 (1.67%)	0	0
ALP increased	3 (5%)	3 (5%)	0	0	0
GGT increased	7 (11.67%)	5 (8.33%)	2 (3.33%)	0	0
Creatine kinase increased	5 (8.33%)	5 (8.33%)	0	0	0
BNP increased	10 (16.67%)	10 (16.67%)	0	0	0

Data are presented as n (%). AST, aspartate aminotransferase; ALT, alanine aminotransferase; ALP, alkaline phosphatase, GGT, gamma-glutamyl transferase; BNP, brain natriuretic peptide.

Table 5: **Summary of adverse events by severity.**

pre- and 17 post-treatment biopsies were collected and implemented using RNA sequencing (Table S7). First, the differentially expressed genes (DEGs) between MPR and non-MPR, PR and non-PR groups were analyzed. The results showed 59 DEGs in both groups (Fig. 3A and B), which were considered the most relevant differential genes with clinical benefits. KEGG pathway analysis revealed that these 59 DEGs were mainly related to metabolism (Fig. 3C). The correlation of these 59 DEGs with survival was analyzed in the TCGA esophageal cancer cohort, and it was found that patients with high expression of PRDM5 and FSIP2 had longer survival (Fig. 3D and E). These results were validated in our own cohort (Fig. S3A and B).

Next, the DEGs of MPR, non-MPR, PR and non-PR patients pre- and post-treatment were analyzed and it was found that the DEGs specifically shared by MPR and PR patients, non-MPR and non-PR, and all patients were 114, 367 and 109, respectively (Fig. 3F–J). These genes were mainly related to the signaling pathways of immunity, metabolism and intracellular signal transduction (Fig. 3K–M). It was suggested that neoadjuvant therapy can modulate the tumor immune microenvironment and tumor cell metabolism. The regulated metabolic pathways are mainly amino acid metabolism and fatty acid metabolism, including histidine metabolism, glutathione metabolism and arachidonic acid metabolism. Glutathione and arachidonic acid enhanced the activity of T cell,[50,51] and both pathways were down-regulated in MPR and PR patients after treatment. This suggests that T cells may be more active in the tumor microenvironment in MPR and PR

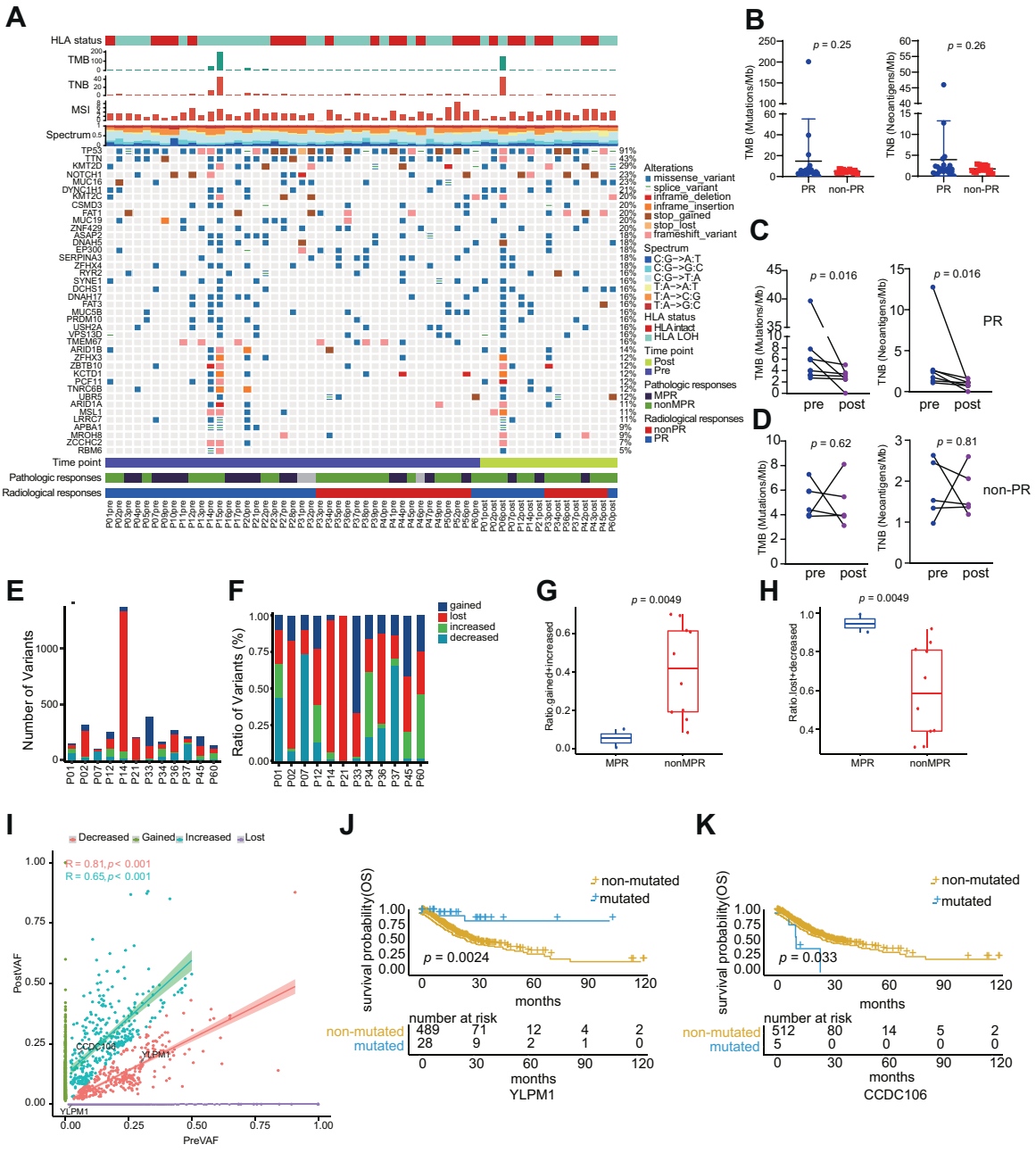

***Fig. 2:* Genomic characteristics of tumors pre- and post-neoadjuvant therapy.** (A) The genomic landscape of ESCC patients treated with neoadjuvant therapy. The state of HLA was shown in top track. The values of TMB, TNB and MSI of each patient were shown in top histogram. The mutation spectrum of each patient was shown under the value of MSI. The distribution of non-synonymous driver mutation events from patients were shown in center heatmap; The bottom tracks are the treatment time, pathologic responses and radiological responses. (B) Comparison of TMB and TNB between patients with PR and non-PR. (C) and (D) Comparison of TMB (C) and TNB (D) pre- and post-treatment in PR and non-PR patients, respectively. (E) and (F) Number of variants (E) and ratio of variants in tumors from pre- and post-treatment biopsies. (G) and (H) Comparison of gained plus increased (G) and lost plus decreased (H) ratio of variants between patients with MPR and non-MPR. (I) Correlation of the VAF of mutations in pre and post treatment samples. (J) and (K) Kaplan–Meier curves of OS comparing the mutation status of YLPM1 (J) and CCDC106 (K) from esophageal cancer patients in TCGA.

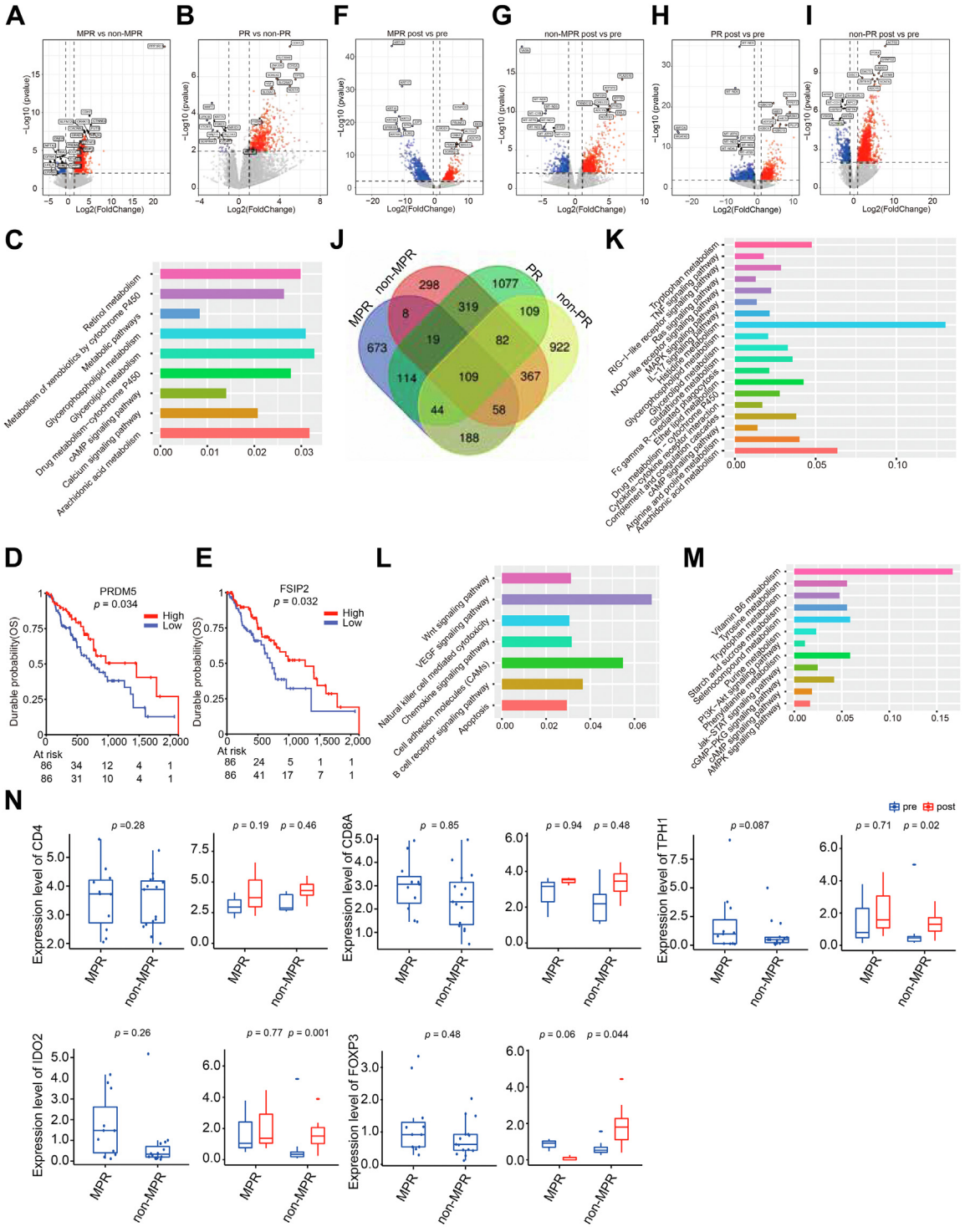

Fig. 3: **Transcriptome analysis and changes during neoadjuvant therapy.** (A) and (B) Volcano plot showing DEGs between MPR and non-MPR (A), PR and non-PR (B). (C) KEGG function enrichment analysis for genes significantly changed in both MPR vs non-MPR and PR vs non-PR groups. (D) and (E) Kaplan–Meier curves of OS comparing the expression levels of PRDM5 (D) and FSIP2 (E) in the TCGA esophageal cancer cohort. (F) To (I) Volcano plot showing DEGs in MPR group (F), non-MPR group (G), PR group (H) and non-PR group (I) pre- and post-treatment. (J) Venn diagrams showing the overlap in genes significantly changed in MPR group, non-MPR group, PR group and non-PR group pre- and post-treatment. (K) To (M) KEGG function enrichment analysis for genes significantly changed in only MPR and PR group

patients after treatment, which may allow them to benefit from treatment.

As neoadjuvant therapy can modulate immune-related pathways in patients with ESCC, immune-related genes were further analyzed. The result was shown in Fig. S3C. It was found that immune-activated genes such as CD4 and CD8a increased in both responders and non-responders, while immunosuppressive genes such as TPH1, IDO2 and Foxp3 also increased in non-responders (Fig. 3N and Fig. S3D).

Increased immunosuppressive cells are responsible for drug resistance during neoadjuvant treatment

Because the expression of immune genes was affected by neoadjuvant therapy, we subsequently hypothesized that neoadjuvant therapy can induce tumor microenvironmental sculpting associated with response. To study the state of TME and its changes pre-and post-treatment, different immune-related signatures were analyzed. The results showed that cytolytic and naïve T-cell signatures increased in both responders and non-responders. However, the T-cell exhaustion signature was close to significantly increased in non-responders (Fig. 4A and B and Fig. S4A).

To further verify this phenomenon, abundance of 12 major immune cells was evaluated by ImmucellAI. At baseline, the CD4 T cells were significantly higher in patients with MPR, while neutrophils were significantly higher in patients with non-MPR (Fig. 4C and Fig. S4B). The correlation of CD4 T cells and neutrophils with survival was further analyzed, and it was found that patients with high CD4 T cell levels had longer OS, PFS and DFS than patients with low CD4 T cell levels (Fig. 4D, Fig. S4C and D). Post-treatment, CD4 and CD8 T lymphocytes increased in both responders and non-responders. However, immune-exhausted cells and Tregs also significantly increased in non-MPR patients, which was consistent with previous analyses of immune genes and signatures (Fig. 4E and Fig. S4E).

To further demonstrate the effect of neoadjuvant therapy on tumor microenvironment, the proportion of CD8 T cells and Tregs in two patients, MPR/PR and non-MPR/PD, were detected using mIF. It was found that CD8 T lymphocytes increased in both two patients post-treatment, while Treg decreased in MPR/PR patient and increased in non-MPR/PD patient (Fig. 4F–H).

The expression levels of IFN-γ, Gal.1 and LAMP3 in serum can predict the efficacy and prognosis of patients

Recent studies have shown that serum proteins can predict the efficacy and adverse effects of immunotherapy combined with chemotherapy.[52–54] However, the potential role of serum protein levels in ESCC has not yet been established. To identify markers that can predict the efficacy and adverse effects of immunotherapy combined with chemotherapy in patients with ESCC, serum samples were collected from 47 patients at baseline, and then detected with Olink-PEA technology (Fig. 5A and Table S8).

The volcano plot of the expression of 92 proteins in these 47 patients was shown in Fig. S5A and B. In patients with MPR, the expression level of TRAIL significantly increased, and IL18 significantly decreased. In patients with PR, the expression of Gal.1, CD244 and TNFRSF4 significantly increased. The association of the response rate with the expression level of serum proteins was analyzed, and it was found that six proteins, including IFN-γ, Gal.1, LAMP3, CD244, CCL23 and CXCL1, were able to predict the efficacy of the treatment (Fig. 5B). The prognostic predictive efficacy of these six proteins was analyzed, and it was found that patients with high expression of IFN-γ and LAMP3 and low expression of Gal.1 had a longer OS (Fig. 5C, Fig. S5C–E).

Association between protein expression levels in serum and AEs

Correlations between the expression levels of 92 proteins and 25 adverse effects were analyzed, and the results were shown in Fig. 6A. It was found that some cytokines were significantly associated with multiple AEs, such as IL8, while some AEs were significantly associated with multiple cytokines, such as thrombopenia (Fig. 6B and C). During treatment, some patients experienced serious AEs. To study whether these proteins can predict the serious AEs, the correlation between these 92 proteins and the serious AEs was analyzed. The results showed that 20 proteins were associated with severe AEs (Fig. 6A last one column), of which IL-8 has been reported to be associated with severe AEs in previous study.[55] The correlation between these proteins and the occurrence rate of serious AEs was further analyzed, and it was found that patients with low expression of CD83, TNFRSF4, TNFSF14, VEGFR.2, ADA and ARG1, and high expression of HO-1 were more likely to experienced serious AEs (Fig. 6D).

Combined CD4 T cells and the expression levels of IFN-γ, LAMP3 or Gal.1 in serum could further distinguish responders from non-responders

As both CD4 T cells and the expression levels of IFN-γ, LAMP3 or Gal.1 in serum could predict the efficacy in ESCC patients treated with immunotherapy combined with chemotherapy, whether the integration of these biomarkers could further distinguish responders. As shown in Fig. 7A–C, patients with low proportion of

(K), only non-MPR and non-PR group (L) and all group (M) pre- and post-treatment. (N) Comparison of CD4, CD8A, TPH1, IDO2 and Foxp3 expression between patients with MPR and non-MPR.

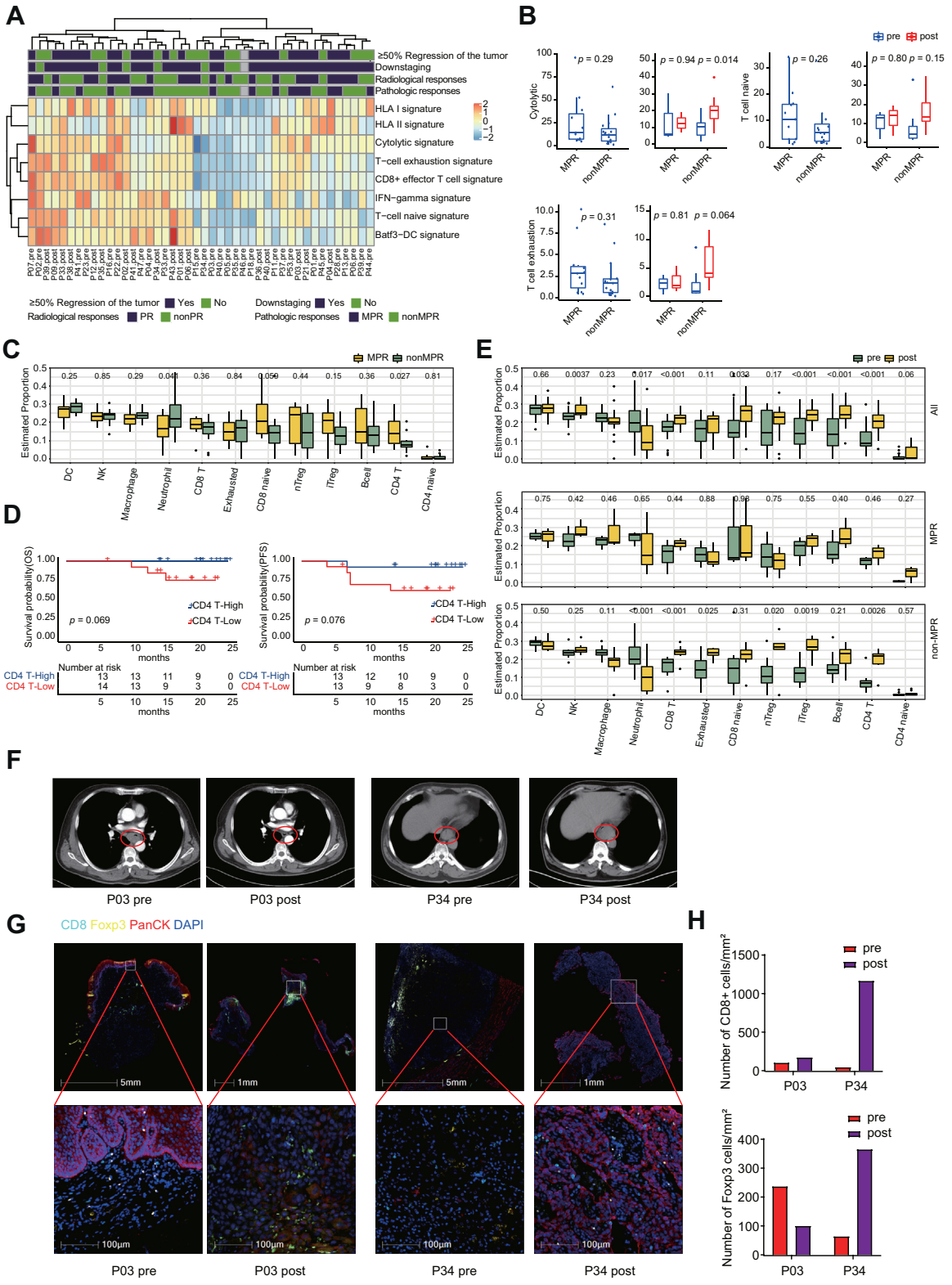

Fig. 4: **Increased immunosuppressive cells are responsible for drug resistance during neoadjuvant treatment.** (A) Heatmap showing the scores of eight immune-related signatures in tumors. (B) Comparison of the scores of Cytolytic, T cell naïve and T cell exhausted signatures pre-

CD4 T cells & high expression of IFN-γ, low proportion of CD4 T cells & low expression of Gal.1, and low proportion of CD4 T cells & high expression of LAMP3 had the lowest OS. Furthermore, we compared the survival of patients with low proportion of CD4 T cells & high expression of IFN-γ, low proportion of CD4 T cells & low expression of Gal.1, or low proportion of CD4 T cells & high expression of LAMP3 with others. It was found that the OS, PFS and DFS were shorter in patients with low proportion of CD4 T cells & high expression of IFN-γ, low proportion of CD4 T cells & low expression of Gal.1, or low proportion of CD4 T cells & high expression of LAMP3 than others (Fig. 7D and E and Fig. S6A–C). More importantly, the predictive efficacy of these combinations was better than that of the individual biomarker (Fig. 7G, Fig. S6D–G). The response rates were further analyzed, and it was found that the response rate of PR was higher in others when compared with low proportion of CD4 T cell & high expression of IFN-γ, low proportion of CD4 T cells & low expression of Gal.1 or low proportion of CD4 T cells & high expression of LAMP3 (Fig. 7H).

Discussion

Currently, neoadjuvant therapy plus esophagectomy is the standard treatment strategy for patients with resectable ESCC. However, platinum-based chemotherapy or combination therapies are highly toxic. Therefore, a less toxic and more effective neoadjuvant treatment regimen is urgently required. In this single-arm phase 2 trial, neoadjuvant therapy toripalimab combined with nab-paclitaxel and S-1 in resectable ESCC had a lower incidence of treatment-related serious AEs (18.3%) with pCR and MPR of 29.09% and 49.09%, respectively. In addition, prognostic biomarkers and tumor ecosystem dynamics during neoadjuvant treatment were analyzed. We observed an association between changes of TMB, TNB and tumor clones with response during treatment. Neoadjuvant therapy can alter the tumor microenvironment and promote the infiltration of CD4 and CD8 T lymphocytes. However, the number of immunosuppressive cells also increased in non-responders. Furthermore, PD-L1 expression, proportion of CD4 T cells and serum levels of IFN-γ, LAMP3 and Gal.1 could predict the efficacy of neoadjuvant treatment, while serum levels of CD83, TNFRSF4, TNFSF14, VEGFR.2, ADA and ARG1 and HO-1 were associated with serious AEs. More importantly, the combination of CD4 T cells and serum levels of IFN-γ, LAMP3 or Gal.1 could further distinguish responders from non-responders.

Overall, the neoadjuvant therapy of toripalimab combined with nab-paclitaxel and S-1 had a favorable safety and feasibility. Serious treatment–related AEs were observed in 18.3% of patients. The incidence was lower than that of previous neoadjuvant regimens, including platinum-based therapy in ESCC, which varied from 32.1% to 48.9%.[56–59] After neoadjuvant therapy, 56 of 60 patients underwent surgery with an R0 resection rate of 98.2%, which was close to that of previously reported neoadjuvant chemoradiotherapy and neoadjuvant ICI combined with chemotherapy, but higher than that of neoadjuvant chemotherapy.[5,58,60] The rate of complications was 30.91% which was lower than the incidence of neoadjuvant chemoradiotherapy and neoadjuvant chemotherapy.[61] Therefore, our results provided evidence that neoadjuvant treatment of toripalimab combined with a less toxic chemotherapy regimen nab-paclitaxel and S-1 was both safe and less toxic.

After neoadjuvant treatment, the pCR rate was 29.09%, which was higher than that of neoadjuvant chemotherapy (10.2%), and similar to that of neoadjuvant chemoradiotherapy (29%) and neoadjuvant ICI combined with chemotherapies (25% and 33.3%).[60,62,63] It has been suggested that pathological response is associated with a better prognosis after neoadjuvant therapy.[64] Among patients with the same pStage, pathological responders had significantly improved 5-year OS with a hazard ratio of 0.24~0.37.[65] In our study, 49.09% MPR and 69.09% ≥ 50% pathological regression were observed. The MPR rate was close to that of previously reported neoadjuvant ICI combined with chemotherapy (50%, 10/20).[60] In addition, downstaging and post-treatment nodal status have been suggested to be important for prognosis.[66–68] In our study, downstaging was observed in 92.73% of patients, which was significantly higher than that previously reported for neoadjuvant chemotherapy, neoadjuvant chemoradiotherapy and neoadjuvant ICI combined with chemotherapy (54%, 61% and 80% respectively).[60,67] Of all patients, 75% achieved ypN0, which was higher than that achieved with neoadjuvant chemoradiotherapy (63.3%).[67] After neoadjuvant therapy, dysphagia was significantly relieved and the quality of life was significantly improved. Therefore, these encouraging results obtained from our study provide clinical evidence for

and post-treatment between patients with MPR and non-MPR. (C) Comparison of the estimated proportion of twelve lymphocytes between patients with MPR and non-MPR at baseline. (D) Kaplan–Meier curves of OS and PFS comparing CD4 T-H and CD4 T-L from pre-treatment biopsies. (E) Comparison of the estimated proportion of twelve lymphocytes pre-and post-treatment in all, MPR and non-MPR patients, respectively. (F) and (G) pre- and post-treatment CT images (F) and mIF staining images of CD8+T and Foxp3+ Treg cells (G) of representative patients with MPR/PR and non-MPR/PD. (H) Comparison of infiltrating CD8+T cells and Foxp3+ Treg between patient with MPR/PR and patient with non-MPR/PD pre- and post-treatment.

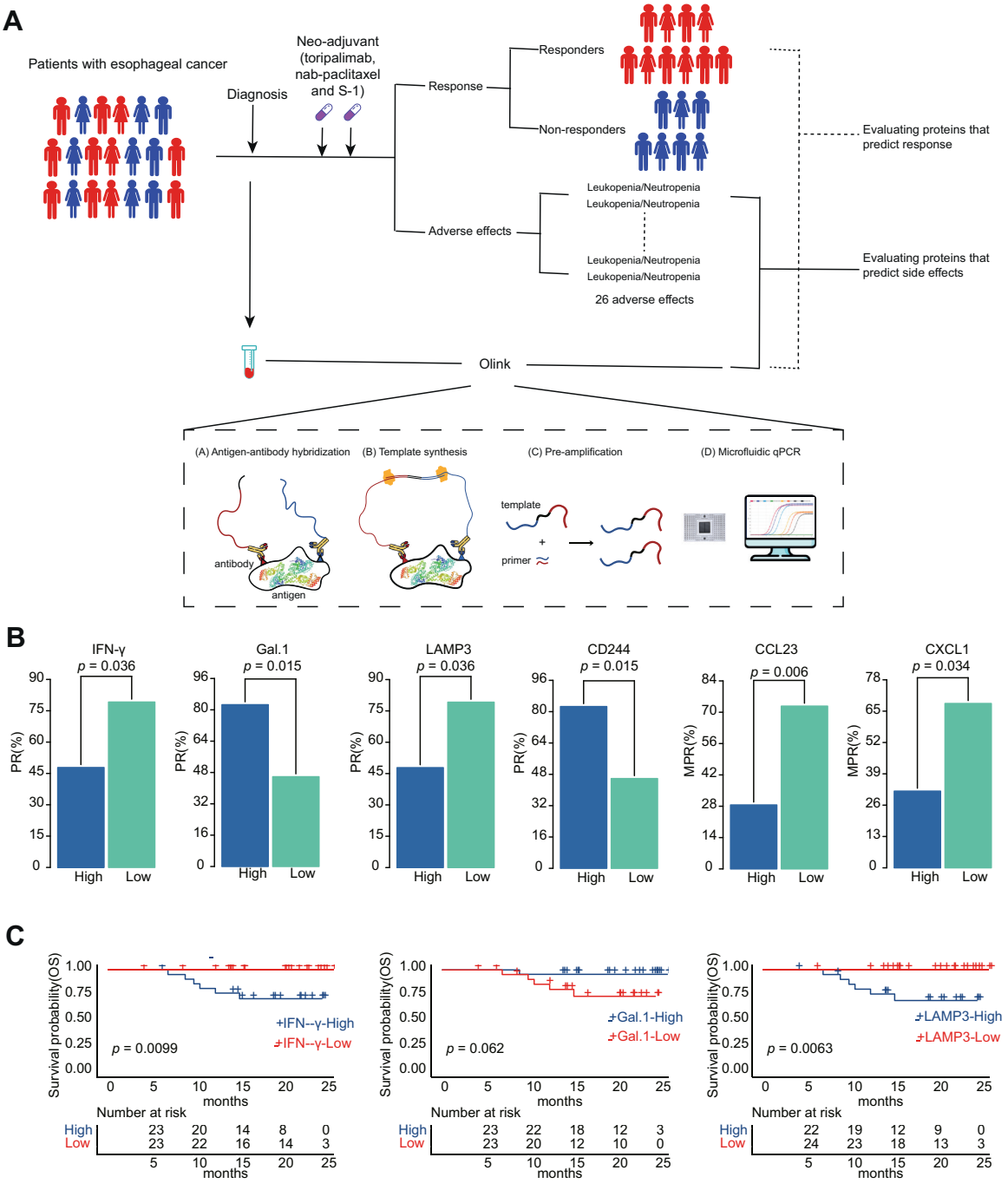

Fig. 5: **The expression levels of IFN-γ, Gal.1 and LAMP3 in serum can predict the efficacy and prognosis of patients.** (A) Schematic diagram of analysis the association of plasma protein with response and adverse effects using PEA technology. (B) Barplots of PR rate between the different groups of IFN-γ, Gal.1, LAMP3, CD244, CCL23 and CXCL1. (C) Kaplan–Meier curves of OS between the different groups of IFN-γ, Gal.1 and LAMP3.

the application of neoadjuvant treatment immunotherapy combined with nab-paclitaxel and S-1.

For older ESCC patients, palliative radiotherapy is usually recommended, but the survival benefit of this therapy is limited.[69,70] Compared with radiotherapy, chemoradiotherapy performed better in local tumor control, distant metastasis and survival for ESCC patients.[69] In a retrospective study, 37.1% of older ESCC

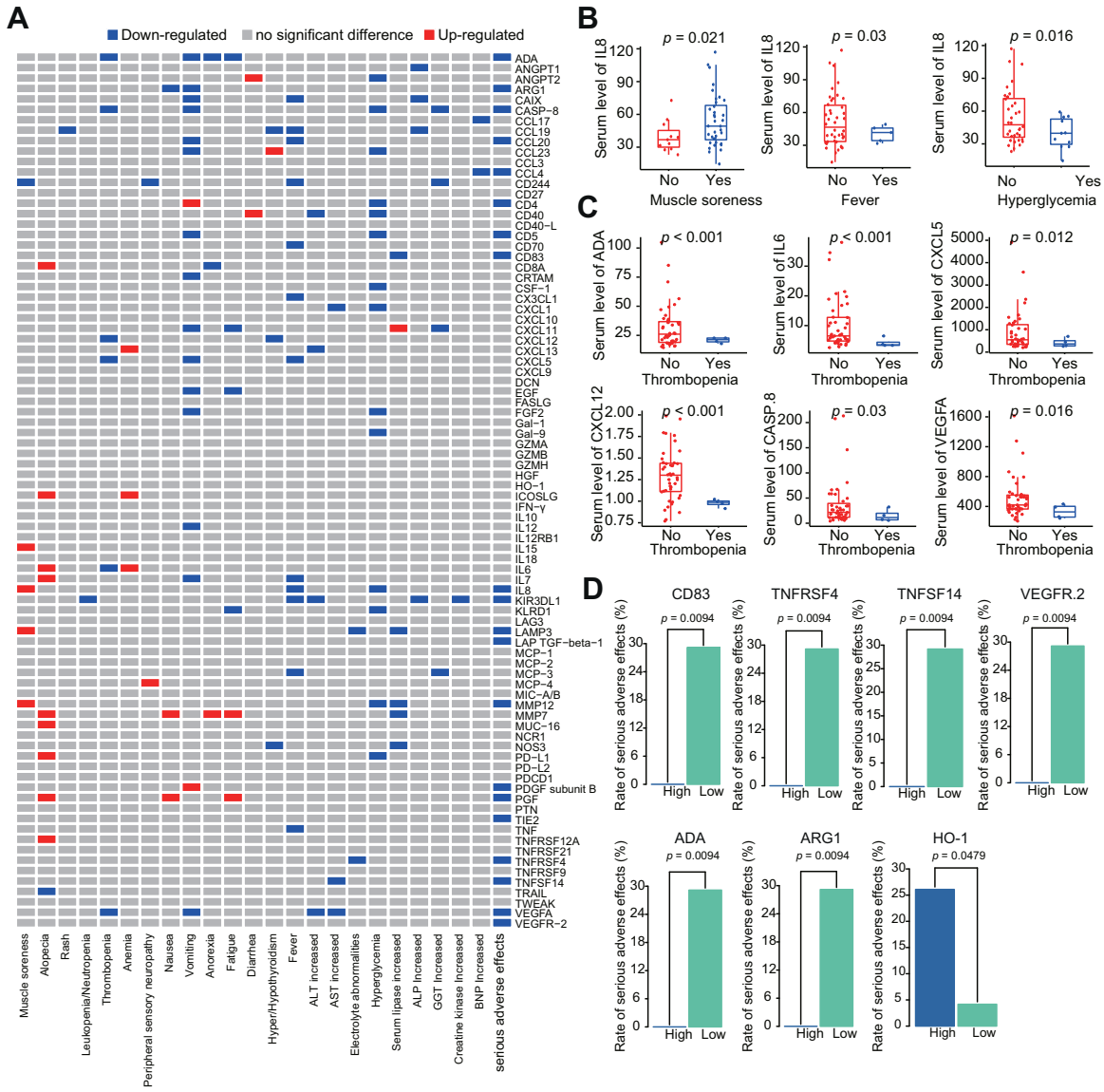

***Fig. 6:* Analysis of the association between protein expression levels in serum and adverse effects.** (A) Heatmap showing the association between serum protein expression levels and adverse effects. (B) Comparison of serum level of IL8 between patients with or without adverse effect of muscle soreness, fever and hyperglycemia. (C) Comparison of serum level of ADA, IL6, CXCL5, CXCL12, CASP.8 and VEGFA between patients with or without adverse effect of thrombopenia. (D) Barplots of serious adverse effects rate between the different groups of CD83, TNFRSF4, TNFSF14, VEGFR2, ADA, ARG1, and HO-1.

patients were found to be treated with definitive concurrent chemoradiotherapy.[71] However, the side effects of chemoradiotherapy are more severe. Study performed by Wu et al. revealed that the hematologic toxicity grade ≥3 was found to be 16.1% (51/317) in older patients with locally advanced ESCC.[72] And a previous study reported that only 33.3% of older patients with esophageal cancer completed the treatment of chemoradiotherapy.[73] Treatment-related mortality is as high as 18% for older patients with locally advanced esophageal cancer.[74] In our study, only 10% older patients experienced the hematologic toxicity greater than grade 3, and no treatment-related mortality was observed. In addition, the pCR and MPR rates in these older patients were 45% and 55%, respectively. These results demonstrated that this neoadjuvant therapy is well-tolerated and effective for older patients with ESCC.

The expression of PD-L1 has served as biomarker for predicting therapeutic effects in many cancers treated with ICIs.[22] However, the predictive value of PD-L1

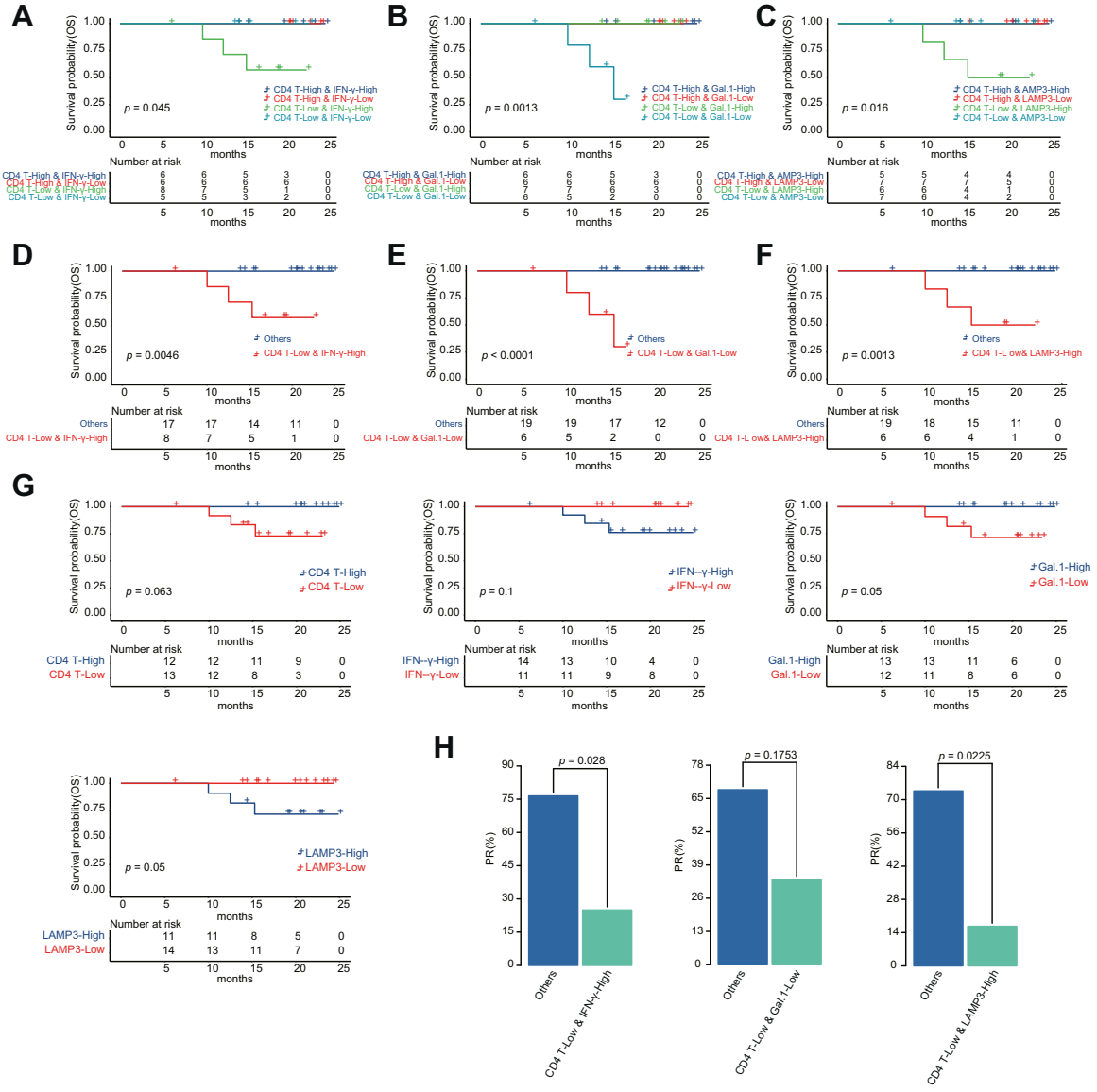

***Fig. 7*: Combination of CD4 T cells and the expression levels of IFN-γ, LAMP3 or Gal.1 in serum could further distinguish responders from non-responders.** (A) Kaplan–Meier curves of OS comparing groups of CD4 T-H & IFN-γ-H, CD4 T-H & IFN-γ-L, CD4 T-L & IFN-γ-H and CD4 T-L & IFN-γ-L. (B) Kaplan–Meier curves of OS comparing groups of CD4 T-H & Gal.1-H, CD4 T-H & Gal.1-L, CD4 T-L & Gal.1-H and CD4 T-L & Gal.1-L. (C) Kaplan–Meier curves of OS comparing groups of CD4 T-H & LAMP3-H, CD4 T-H & LAMP3-L, CD4 T-L & LAMP3-H and CD4 T-L & LAMP3-L. (D) Kaplan–Meier curves of OS comparing groups of CD4 T-L & IFN-γ-H and others. (E) Kaplan–Meier curves of OS comparing groups of CD4 T-L & Gal.1-L and others. (F) Kaplan–Meier curves of OS comparing groups of CD4 T-L & LAMP3-H and others. (G) Kaplan–Meier curves of OS comparing the different groups of CD4 T, IFN-γ, Gal.1 and LAMP3. (H) Barplots of PR rate between the different groups of CD4 T & IFN-γ, CD4 T & Gal.1 and CD4 & LAMP3.

expression in ESCC treated with ICIs or ICIs combined with other therapies remains controversial.[21,75–77] In our study, we observed that PD-L1 expression was significantly higher in patients with PR, and the response rate of PR was significantly higher in patients with a PD-L1 CPS ≥10. During treatment, PD-L1 expression decreased in responders and increased in non-responders. However, the survival analysis was not significant with PD-L1 expression, which was similar to the results of a previous study on ESCC patients treated with immunotherapy combined with chemotherapy.[60] This may be due to the shorter follow-up period.

Multiple studies have verified the predictive efficacy of genomic biomarkers in cancers treated with ICI, especially TMB.[32,78–81] However, their predictive values for ESCC patients treated with ICI combined with

chemotherapy were unclear.[21,60] In our study, these genomic biomarkers were found to be ineffective in predicting efficacy. Although patients with high TMB and TNB had a longer OS, there was no significant difference, which is consistent with previous reports.[60] During treatment, we observed that TMB, TNB and tumor clone evolution were associated with response which was similar to the results of a previous study.[42] New mutations were selected under immunological pressure, which may result in the drug resistance.

The immune landscape of the ESCC tumor microenvironment was an immunosuppressive state which was dominated by exhausted T cells, natural killer (NK) cells, Tregs, macrophages and tolerogenic DCs.[21] In our study, the top infiltrating lymphocytes were DCs, NK cells, Macrophages, CD8 T cells and exhausted cells at baseline, which was similar to the findings of a previous study. After treatment, CD4 and CD8 T cells were significantly increased, indicating that neoadjuvant therapy can induce efficient and durable antitumor immunity. However, exhausted cells and Tregs were significantly increased in non-MPR patients. It is well-known that exhausted cells and Tregs can inhibit the cytolytic function of T lymphocytes, thereby promoting the immunosuppressive microenvironment.[82] These results suggested that the induction of exhausted cells and Tregs may result in the ineffective immunotherapy. However, the mechanisms by which neoadjuvant therapy induces exhausted cells and Tregs in non-responders required further study. Furthermore, combinations with drugs that specifically target these immunosuppressive cells may reactivate antitumor immune responses, thereby further benefiting non-responders.

Previous studies have demonstrated the predictive value of circulating biomarkers for both the efficacy and serious AEs of immunotherapy.[52,53] In our study, the expression of 92 proteins was detected using the Olink multiplex immuno-oncology panel and correlated with efficacy and AEs. Three serum proteins, including IFN-γ, were associated with efficacy and prognosis. Patients with lower serum levels of IFN-γ had clinical benefits, which was consistent with the findings of a previous report.[83] In addition, 20 serum proteins were associated with serious AEs, including the previously reported IL8.[55] However, the mechanisms underlying the efficacy and AEs of these plasma proteins were unclear, and further research was needed.

Previous studies have shown that a single biomarker cannot effectively predict efficacy and prognosis, and the current strategy is to combine different markers.[84–86] Our results showed that combined CD4 T lymphocytes and serum levels of IFN-γ, LAMP3 or Gal.1 could further distinguish responders from non-responders. However, this conclusion was not further validated because of the small number of patients who underwent both RNA-seq and Olink multiplex immune-oncology panel, and needed to be further verified.

The current study is subjected to certain limitations. First, as a pilot study, no control arm was included. The direct comparison with results from other studies could only be suggestive without confirmative information. Second, the follow-up period was short and the mOS was not reached at present. In the future, we will timely report the results of long-term follow-up. In addition, others long-term follow-up studies will be necessary to further examine whether neoadjuvant immunotherapy combined with chemotherapy can provides a long-term survival benefit for patients with resectable ESCC.

In conclusion, neoadjuvant therapy of toripalimab combined with nab-paclitaxel and S-1 was less toxic and resulted in a significant pathological response and downstaging in patients with resectable ESCC, indicating that this regimen is a potential treatment strategy for such patients. Biomarkers for response and serious AEs were identified, and the tumor and microenvironment ecosystem dynamics were clarified. These results provided insight into the underlying mechanisms that contributed to the response to immunotherapy combined with chemotherapy in patients with resectable ESCC. However, further studies are needed to validate these findings.

Contributors

G.Q. Zhang: Conceptualization, Formal analysis, Funding acquisition, Methodology, Writing–original draft. J. Yuan: Formal analysis, Methodology, Writing–original draft. C.H. Pan: Formal analysis, Methodology, Writing–original draft. Q. Xu: Formal analysis. X.L. Cui: Formal analysis. J. Zhang: Validation, Writing—reviewing & editing. M.L. Liu: Validation, Writing—reviewing & editing. Z.G. Song: Validation, Writing—reviewing & editing. L.L. Wu: Validation, Writing—reviewing & editing. D.F. Wu: Validation, Writing—reviewing & editing. H.T. Luo: Conceptualization, Investigation, Validation, Verification of underlying data, Supervision, Writing—reviewing & editing. Y. Hu: Conceptualization, methodology, Investigation, Validation, Writing—reviewing & editing. S.C. Jiao: Conceptualization, methodology, Investigation, Validation, Verification of underlying data, Supervision, Writing—reviewing & editing. B. Yang: Conceptualization, methodology, Investigation, Validation, Verification of underlying data, Supervision, Writing—reviewing & editing.

Data sharing statement

All the analysis data can be found in supplementary table. The raw data generated in this study are not publicly available due to the privacy protection policy of personal medical data at our institution, but are available from the corresponding author on reasonable request.

Declaration of interests

Dr. Zhang reports grants from Major projects of the ministry of science and technology of the 13th five-year plan of China, during the conduct of the study; non-financial support from Shanghai Junshi Bioscience Co., Ltd, outside the submitted work. The remaining authors have nothing to disclose.

Acknowledgments

We would like to thank Shanghai Junshi Bioscience Co., Ltd for providing toripalimab for this study.

Appendix A. Supplementary data

Supplementary data related to this article can be found at https://doi.org/10.1016/j.ebiom.2023.104515.

References

1 Park S, Joung JG, Min YW, et al. Paired whole exome and transcriptome analyses for the immunogenomic changes during concurrent chemoradiotherapy in esophageal squamous cell carcinoma. *J Immunother Cancer*. 2019;7(1):128.
2 Torre LA, Bray F, Siegel RL, Ferlay J, Lortet-Tieulent J, Jemal A. Global cancer statistics, 2012. *CA Cancer J Clin*. 2015;65(2):87–108.
3 Watanabe M, Otake R, Kozuki R, et al. Recent progress in multidisciplinary treatment for patients with esophageal cancer. *Surg Today*. 2020;50(1):12–20.
4 Rustgi AK, El-Serag HB. Esophageal carcinoma. *N Engl J Med*. 2014;371(26):2499–2509.
5 Medical Research Council Oesophageal Cancer Working G. Surgical resection with or without preoperative chemotherapy in oesophageal cancer: a randomised controlled trial. *Lancet*. 2002;359(9319):1727–1733.
6 Allum WH, Stenning SP, Bancewicz J, Clark PI, Langley RE. Long-term results of a randomized trial of surgery with or without preoperative chemotherapy in esophageal cancer. *J Clin Oncol*. 2009;27(30):5062–5067.
7 Mariette C, Dahan L, Mornex F, et al. Surgery alone versus chemoradiotherapy followed by surgery for stage I and II esophageal cancer: final analysis of randomized controlled phase III trial FFCD 9901. *J Clin Oncol*. 2014;32(23):2416–2422.
8 Chan KKW, Saluja R, Delos Santos K, et al. Neoadjuvant treatments for locally advanced, resectable esophageal cancer: a network meta-analysis. *Int J Cancer*. 2018;143(2):430–437.
9 Andrews LP, Yano H, Vignali DAA. Inhibitory receptors and ligands beyond PD-1, PD-L1 and CTLA-4: breakthroughs or backups. *Nat Immunol*. 2019;20(11):1425–1434.
10 Zhang H, Dai Z, Wu W, et al. Regulatory mechanisms of immune checkpoints PD-L1 and CTLA-4 in cancer. *J Exp Clin Cancer Res*. 2021;40(1):184.
11 Sharma P, Siddiqui BA, Anandhan S, et al. The next decade of immune checkpoint therapy. *Cancer Discov*. 2021;11(4):838–857.
12 Baba Y, Nomoto D, Okadome K, et al. Tumor immune microenvironment and immune checkpoint inhibitors in esophageal squamous cell carcinoma. *Cancer Sci*. 2020;111(9):3132–3141.
13 Morad G, Helmink BA, Sharma P, Wargo JA. Hallmarks of response, resistance, and toxicity to immune checkpoint blockade. *Cell*. 2021;184(21):5309–5337.
14 Chuang J, Chao J, Hendifar A, Klempner SJ, Gong J. Checkpoint inhibition in advanced gastroesophageal cancer: clinical trial data, molecular subtyping, predictive biomarkers, and the potential of combination therapies. *Transl Gastroenterol Hepatol*. 2019;4:63.
15 Pelosof L, Saung MT, Donoghue M, et al. Benefit-risk summary of nivolumab for the treatment of patients with unresectable advanced, recurrent, or metastatic esophageal squamous cell carcinoma after prior fluoropyrimidine- and platinum-based chemotherapy. *Oncologist*. 2021;26(4):318–324.
16 Galluzzi L, Humeau J, Buque A, Zitvogel L, Kroemer G. Immunostimulation with chemotherapy in the era of immune checkpoint inhibitors. *Nat Rev Clin Oncol*. 2020;17(12):725–741.
17 Wang YJ, Fletcher R, Yu J, Zhang L. Immunogenic effects of chemotherapy-induced tumor cell death. *Genes Dis*. 2018;5(3):194–203.
18 Fabian KP, Wolfson B, Hodge JW. From immunogenic cell death to immunogenic modulation: select chemotherapy regimens induce a spectrum of immune-enhancing activities in the tumor microenvironment. *Front Oncol*. 2021;11:728018.
19 Huang B, Shi H, Gong X, et al. Comparison of efficacy and safety between pembrolizumab combined with chemotherapy and simple chemotherapy in neoadjuvant therapy for esophageal squamous cell carcinoma. *J Gastrointest Oncol*. 2021;12(5):2013–2021.
20 Oun R, Moussa YE, Wheate NJ. The side effects of platinum-based chemotherapy drugs: a review for chemists. *Dalton Trans*. 2018;47(19):6645–6653.
21 Yang G, Su X, Yang H, et al. Neoadjuvant programmed death-1 blockade plus chemotherapy in locally advanced esophageal squamous cell carcinoma. *Ann Transl Med*. 2021;9(15):1254.
22 Doroshow DB, Bhalla S, Beasley MB, et al. PD-L1 as a biomarker of response to immune-checkpoint inhibitors. *Nat Rev Clin Oncol*. 2021;18(6):345–362.
23 Petitprez F, Meylan M, de Reynies A, Sautes-Fridman C, Fridman WH. The tumor microenvironment in the response to immune checkpoint blockade therapies. *Front Immunol*. 2020;11:784.
24 Rosen RD, Sapra A. TNM classification. Treasure Island (FL). In: *StatPearls*. 2022.
25 Daud AI, Wolchok JD, Robert C, et al. Programmed death-ligand 1 expression and response to the anti-programmed death 1 antibody pembrolizumab in melanoma. *J Clin Oncol*. 2016;34(34):4102–4109.
26 Chen Y, Chen Y, Shi C, et al. SOAPnuke: a MapReduce acceleration-supported software for integrated quality control and preprocessing of high-throughput sequencing data. *Gigascience*. 2018;7(1):1–6.
27 Li H, Durbin R. Fast and accurate short read alignment with Burrows-Wheeler transform. *Bioinformatics*. 2009;25(14):1754–1760.
28 Danecek P, Bonfield JK, Liddle J, et al. Twelve years of SAMtools and BCFtools. *Gigascience*. 2021;10(2):giab008.
29 Faust GG, Hall IM. SAMBLASTER: fast duplicate marking and structural variant read extraction. *Bioinformatics*. 2014;30(17):2503–2505.
30 McLaren W, Gil L, Hunt SE, et al. The ensembl variant effect predictor. *Genome Biol*. 2016;17(1):122.
31 Cingolani P, Platts A, Wang le L, et al. A program for annotating and predicting the effects of single nucleotide polymorphisms, SnpEff: SNPs in the genome of Drosophila melanogaster strain w1118; iso-2; iso-3. *Fly (Austin)*. 2012;6(2):80–92.
32 Fang W, Jin H, Zhou H, et al. Intratumoral heterogeneity as a predictive biomarker in anti-PD-(L)1 therapies for non-small cell lung cancer. *Mol Cancer*. 2021;20(1):37.
33 Shukla SA, Rooney MS, Rajasagi M, et al. Comprehensive analysis of cancer-associated somatic mutations in class I HLA genes. *Nat Biotechnol*. 2015;33(11):1152–1158.
34 McGranahan N, Rosenthal R, Hiley CT, et al. Allele-specific HLA loss and immune escape in lung cancer evolution. *Cell*. 2017;171(6):1259–1271.e1211.
35 Nielsen M, Andreatta M. NetMHCpan-3.0; improved prediction of binding to MHC class I molecules integrating information from multiple receptor and peptide length datasets. *Genome Med*. 2016;8(1):33.
36 Szolek A, Schubert B, Mohr C, Sturm M, Feldhahn M, Kohlbacher O. OptiType: precision HLA typing from next-generation sequencing data. *Bioinformatics*. 2014;30(23):3310–3316.
37 Jia P, Yang X, Guo L, et al. MSIsensor-pro: fast, accurate, and matched-normal-sample-free detection of microsatellite instability. *Genomics Proteomics Bioinformatics*. 2020;18(1):65–71.
38 Roth A, Khattra J, Yap D, et al. PyClone: statistical inference of clonal population structure in cancer. *Nat Methods*. 2014;11(4):396–398.
39 Bray NL, Pimentel H, Melsted P, Pachter L. Near-optimal probabilistic RNA-seq quantification. *Nat Biotechnol*. 2016;34(5):525–527.
40 Love MI, Huber W, Anders S. Moderated estimation of fold change and dispersion for RNA-seq data with DESeq2. *Genome Biol*. 2014;15(12):550.
41 Bu D, Luo H, Huo P, et al. KOBAS-i: intelligent prioritization and exploratory visualization of biological functions for gene enrichment analysis. *Nucleic Acids Res*. 2021;49(W1):W317–W325.
42 Riaz N, Havel JJ, Makarov V, et al. Tumor and microenvironment evolution during immunotherapy with nivolumab. *Cell*. 2017;171(4):934–949.e916.
43 Miao YR, Zhang Q, Lei Q, et al. A unique method for comprehensive T-cell subsets abundance prediction and its application in cancer immunotherapy. *Adv Sci*. 2020;7(7):1902880.
44 Assarsson E, Lundberg M, Holmquist G, et al. Homogenous 96-plex PEA immunoassay exhibiting high sensitivity, specificity, and excellent scalability. *PLoS One*. 2014;9(4):e95192.
45 Klevebro F, Alexandersson von Dobeln G, Wang N, et al. A randomized clinical trial of neoadjuvant chemotherapy versus neoadjuvant chemoradiotherapy for cancer of the oesophagus or gastro-oesophageal junction. *Ann Oncol*. 2016;27(4):660–667.
46 Anderegg MCJ, van der Sluis PC, Ruurda JP, et al. Preoperative chemoradiotherapy versus perioperative chemotherapy for patients with resectable esophageal or gastroesophageal junction adenocarcinoma. *Ann Surg Oncol*. 2017;24(8):2282–2290.
47 1058P A single-centre, prospective, open-label, single-arm trial of toripalimab with nab-paclitaxel and S-1 as a neoadjuvant therapy for esophageal squamous cell carcinoma (ESCC). *Ann Oncol*. 2020;31:S722.
48 Cui Y, Chen H, Xi R, et al. Whole-genome sequencing of 508 patients identifies key molecular features associated with poor prognosis in esophageal squamous cell carcinoma. *Cell Res*. 2020;30(10):902–913.

49 Cancer Genome Atlas Research N, Analysis Working Group, Asan U, et al. Integrated genomic characterization of oesophageal carcinoma. *Nature*. 2017;541(7636):169–175.
50 Mak TW, Grusdat M, Duncan GS, et al. Glutathione primes T cell metabolism for inflammation. *Immunity*. 2017;46(6):1089–1090.
51 Das UN. Bioactive lipids as modulators of immune check point inhibitors. *Med Hypotheses*. 2020;135:109473.
52 Yuen KC, Liu LF, Gupta V, et al. High systemic and tumor-associated IL-8 correlates with reduced clinical benefit of PD-L1 blockade. *Nat Med*. 2020;26(5):693–698.
53 Tyan K, Baginska J, Brainard M, et al. Cytokine changes during immune-related adverse events and corticosteroid treatment in melanoma patients receiving immune checkpoint inhibitors. *Cancer Immunol Immunother*. 2021;70(8):2209–2221.
54 Sanmamed MF, Perez-Gracia JL, Schalper KA, et al. Changes in serum interleukin-8 (IL-8) levels reflect and predict response to anti-PD-1 treatment in melanoma and non-small-cell lung cancer patients. *Ann Oncol*. 2017;28(8):1988–1995.
55 von Itzstein MS, Khan S, Gerber DE. Investigational biomarkers for checkpoint inhibitor immune-related adverse event prediction and diagnosis. *Clin Chem*. 2020;66(6):779–793.
56 Kanda M, Koike M, Iwata N, et al. An open-label single-arm phase II study of treatment with neoadjuvant S-1 plus cisplatin for clinical stage III squamous cell carcinoma of the esophagus. *Oncologist*. 2020;25(11):e1650–e1654.
57 Ohnuma H, Sato Y, Hayasaka N, et al. Neoadjuvant chemotherapy with docetaxel, nedaplatin, and fluorouracil for resectable esophageal cancer: a phase II study. *Cancer Sci*. 2018;109(11):3554–3563.
58 Yang H, Liu H, Chen Y, et al. Neoadjuvant chemoradiotherapy followed by surgery versus surgery alone for locally advanced squamous cell carcinoma of the esophagus (NEOCRTEC5010): a phase III multicenter, randomized, open-label clinical trial. *J Clin Oncol*. 2018;36(27):2796–2803.
59 Nomura M, Kato K, Ando N, et al. Comparison between neoadjuvant chemotherapy followed by surgery and definitive chemoradiotherapy for overall survival in patients with clinical Stage II/III esophageal squamous cell carcinoma (JCOG1406-A). *Jpn J Clin Oncol*. 2017;47(6):480–486.
60 Yang W, Xing X, Yeung SJ, et al. Neoadjuvant programmed cell death 1 blockade combined with chemotherapy for resectable esophageal squamous cell carcinoma. *J Immunother Cancer*. 2022;10(1):e003497.
61 Markar SR, Noordman BJ, Mackenzie H, et al. Multimodality treatment for esophageal adenocarcinoma: multi-center propensity-score matched study. *Ann Oncol*. 2017;28(3):519–527.
62 Castoro C, Scarpa M, Cagol M, et al. Nodal metastasis from locally advanced esophageal cancer: how neoadjuvant therapy modifies their frequency and distribution. *Ann Surg Oncol*. 2011;18(13):3743–3754.
63 Shen D, Chen Q, Wu J, Li J, Tao K, Jiang Y. The safety and efficacy of neoadjuvant PD-1 inhibitor with chemotherapy for locally advanced esophageal squamous cell carcinoma. *J Gastrointest Oncol*. 2021;12(1):1–10.
64 Pataer A, Kalhor N, Correa AM, et al. Histopathologic response criteria predict survival of patients with resected lung cancer after neoadjuvant chemotherapy. *J Thorac Oncol*. 2012;7(5):825–832.
65 Matsuda S, Kawakubo H, Okamura A, et al. Prognostic significance of stratification using pathological stage and response to neoadjuvant chemotherapy for esophageal squamous cell carcinoma. *Ann Surg Oncol*. 2021;28(13):8438–8447.
66 Kamarajah SK, Navidi M, Wahed S, et al. Significance of neoadjuvant downstaging in carcinoma of esophagus and gastro-esophageal junction. *Ann Surg Oncol*. 2020;27(9):3182–3192.
67 Jiang D, Wang H, Song Q, et al. Comparison of the prognostic difference between ypTNM and equivalent pTNM stages in esophageal squamous cell carcinoma based on the 8th edition of AJCC classification. *J Cancer*. 2020;11(7):1808–1815.
68 Takeda FR, Tustumi F, de Almeida Obregon C, et al. Prognostic value of tumor regression grade based on ryan score in squamous cell carcinoma and adenocarcinoma of esophagus. *Ann Surg Oncol*. 2020;27(4):1241–1247.
69 Herskovic A, Martz K, al-Sarraf M, et al. Combined chemotherapy and radiotherapy compared with radiotherapy alone in patients with cancer of the esophagus. *N Engl J Med*. 1992;326(24):1593–1598.
70 Ajani JA, D'Amico TA, Almhanna K, et al. Esophageal and esophagogastric junction cancers, version 1.2015. *J Natl Compr Canc Netw*. 2015;13(2):194–227.
71 Ji Y, Du X, Tian Y, et al. A phase II study of S-1 with concurrent radiotherapy in elderly patients with esophageal cancer. *Oncotarget*. 2017;8(47):83022–83029.
72 Wu H, Yu Y, Zheng Q, et al. Benefit of chemotherapy based on platinum with definitive radiotherapy in older patients with locally advanced esophageal squamous cell carcinoma. *Radiat Oncol*. 2021;16(1):207.
73 Takeuchi S, Ohtsu A, Doi T, et al. A retrospective study of definitive chemoradiotherapy for elderly patients with esophageal cancer. *Am J Clin Oncol*. 2007;30(6):607–611.
74 Wakui R, Yamashita H, Okuma K, et al. Esophageal cancer: definitive chemoradiotherapy for elderly patients. *Dis Esophagus*. 2010;23(7):572–579.
75 Kawazoe A, Yamaguchi K, Yasui H, et al. Safety and efficacy of pembrolizumab in combination with S-1 plus oxaliplatin as a first-line treatment in patients with advanced gastric/gastroesophageal junction cancer: cohort 1 data from the KEYNOTE-659 phase IIb study. *Eur J Cancer*. 2020;129:97–106.
76 Lee J, Kim B, Jung HA, La Choi Y, Sun JM. Nivolumab for esophageal squamous cell carcinoma and the predictive role of PD-L1 or CD8 expression in its therapeutic effect. *Cancer Immunol Immunother*. 2021;70(5):1203–1211.
77 Cao Y, Qin S, Luo S, et al. Pembrolizumab versus chemotherapy for patients with esophageal squamous cell carcinoma enrolled in the randomized KEYNOTE-181 trial in Asia. *ESMO Open*. 2021;7(1):100341.
78 Jardim DL, Goodman A, de Melo Gagliato D, Kurzrock R. The challenges of tumor mutational burden as an immunotherapy biomarker. *Cancer Cell*. 2021;39(2):154–173.
79 Montesion M, Murugesan K, Jin DX, et al. Somatic HLA class I loss is a widespread mechanism of immune evasion which refines the use of tumor mutational burden as a biomarker of checkpoint inhibitor response. *Cancer Discov*. 2021;11(2):282–292.
80 Wang P, Chen Y, Wang C. Beyond tumor mutation burden: tumor neoantigen burden as a biomarker for immunotherapy and other types of therapy. *Front Oncol*. 2021;11:672677.
81 Cui G. The mechanisms leading to distinct responses to PD-1/PD-L1 blockades in colorectal cancers with different MSI statuses. *Front Oncol*. 2021;11:573547.
82 Saleh R, Elkord E. Treg-mediated acquired resistance to immune checkpoint inhibitors. *Cancer Lett*. 2019;457:168–179.
83 Huang AC, Postow MA, Orlowski RJ, et al. T-cell invigoration to tumour burden ratio associated with anti-PD-1 response. *Nature*. 2017;545(7652):60–65.
84 Shi Y, Lei Y, Liu L, et al. Integration of comprehensive genomic profiling, tumor mutational burden, and PD-L1 expression to identify novel biomarkers of immunotherapy in non-small cell lung cancer. *Cancer Med*. 2021;10(7):2216–2231.
85 Liu D, Schilling B, Liu D, et al. Integrative molecular and clinical modeling of clinical outcomes to PD1 blockade in patients with metastatic melanoma. *Nat Med*. 2019;25(12):1916–1927.
86 Lin Z, Zhang Y, Zhang L. Construction of an integrated prognostic classifier model for predicting the efficacy of immune checkpoint inhibitor therapy in non-small cell lung cancer. *Cancer Commun*. 2020;40(8):370–373.